Input-output analysis of high-speed turbulent jet noise

Jinah Jeun

Postdoctoral Fellow, Center for Turbulence Research, Stanford University

Acknowledgements:

Joseph Nichols (University of Minnesota)

Mihailo Jovanovic, Armin Zare (University of Southern California)

Sanjiva Lele, Gary Wu (Stanford University)

AMS Seminar Series, NASA Ames Research Center

March 28, 2019

Jet noise

- Major source of aviation noise
- Hazard to people working in close proximity

→ Stringent noise regulations

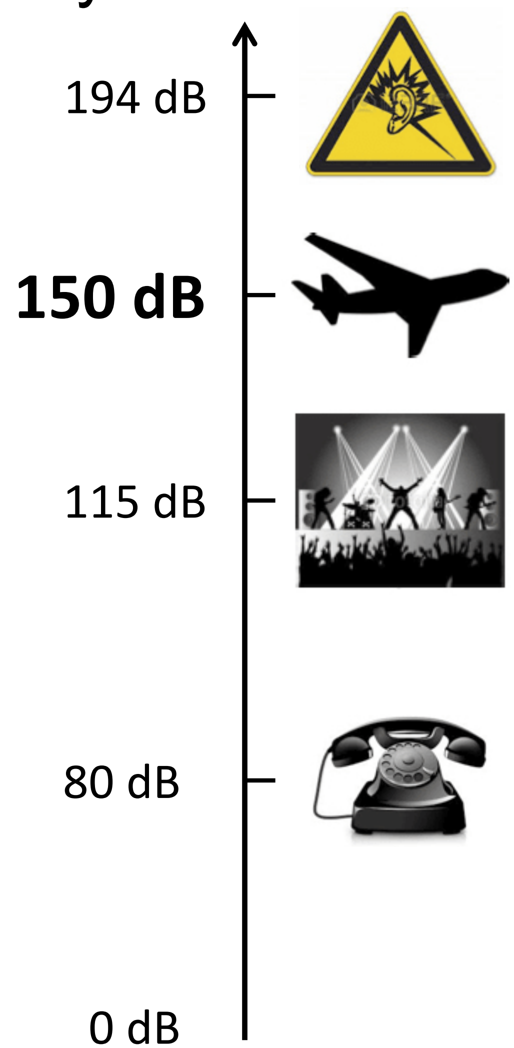

Jet noise

- Predicting jet noise is challenging
  - Acoustic energy << Aerodynamic energy
- Understanding physics of turbulence helps to predict noise
  - Turbulence is chaotic, but noise is organized!

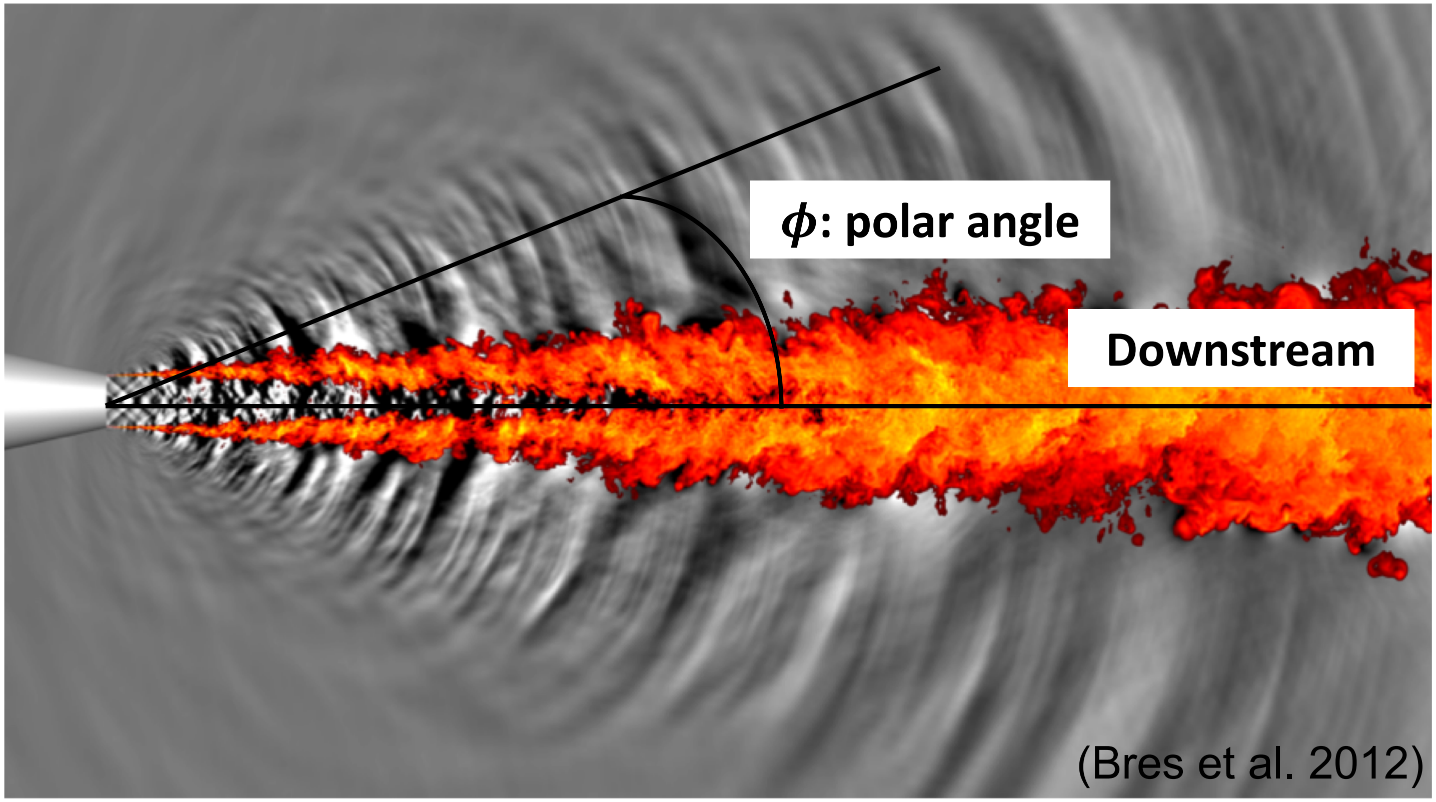

Acoustic sources

- Acoustic analogy (**Statistical** description)
  - Lighthill 1952; Ffowcs Williams 1963; Lilley 1974; Goldstein 2003
  - Fine-scale turbulence
- Wavepackets (**Dynamical** description)
  - Mollo-Christensen 1963, 1967
  - Non-compact acoustic sources (instability waves)
    - Parabolized stability equations (PSE)
    - Global mode analysis (Nichols & Lele 2011)
    - Resolvent analysis (Schmid & Henningson 2001; Garnaud et al. 2013)

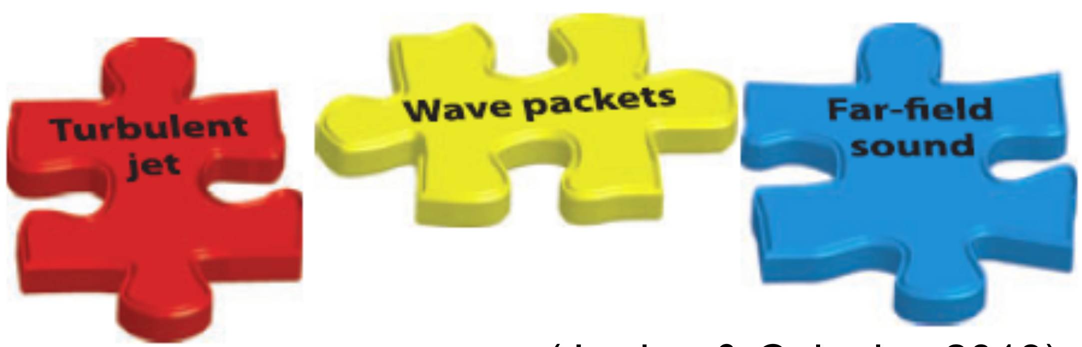

(Jordan & Colonius 2013)

Missing sound?

- PSE or linearized Euler equations (LEE)
  - Recovers sound generation in supersonic jets
    - ✓ Sinha et al. 2014
  - Breaks down for **subsonic** jets & **supersonic heated** jets
    - ✓ Cheung & Lele 2007; Rodriguez et al. 2011; Jordan et al. 2014

Mach 0.9 subsonic jet

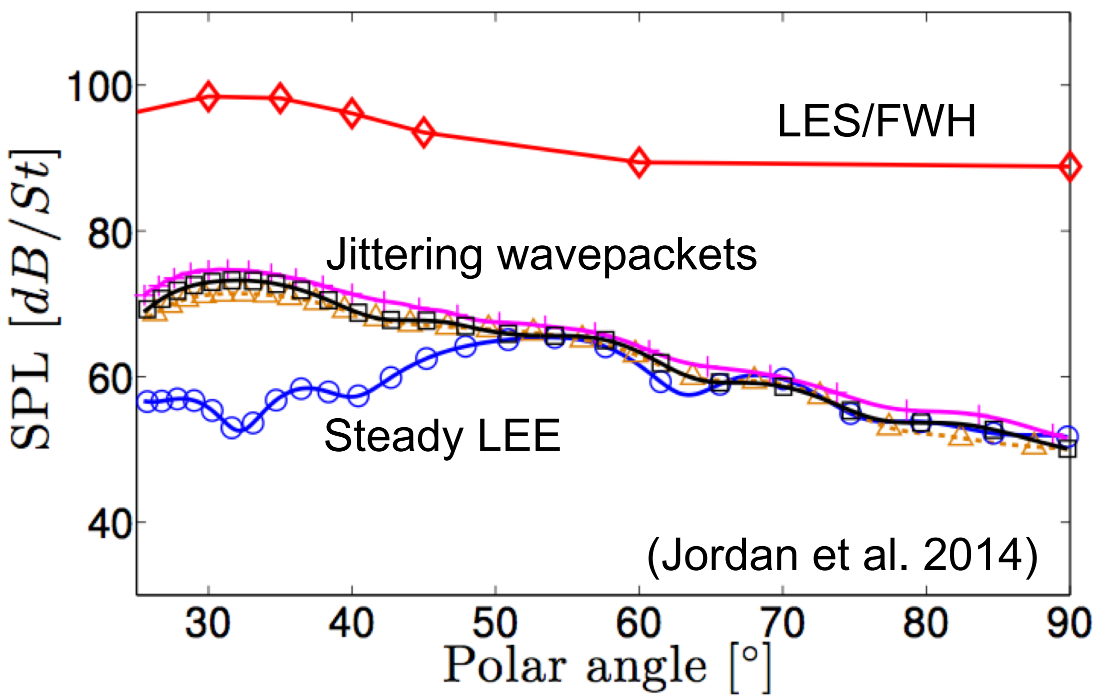

Wavepacket modeling

- Scaled wavepackets can match spectra at all angles

Mach 0.9 subsonic jet

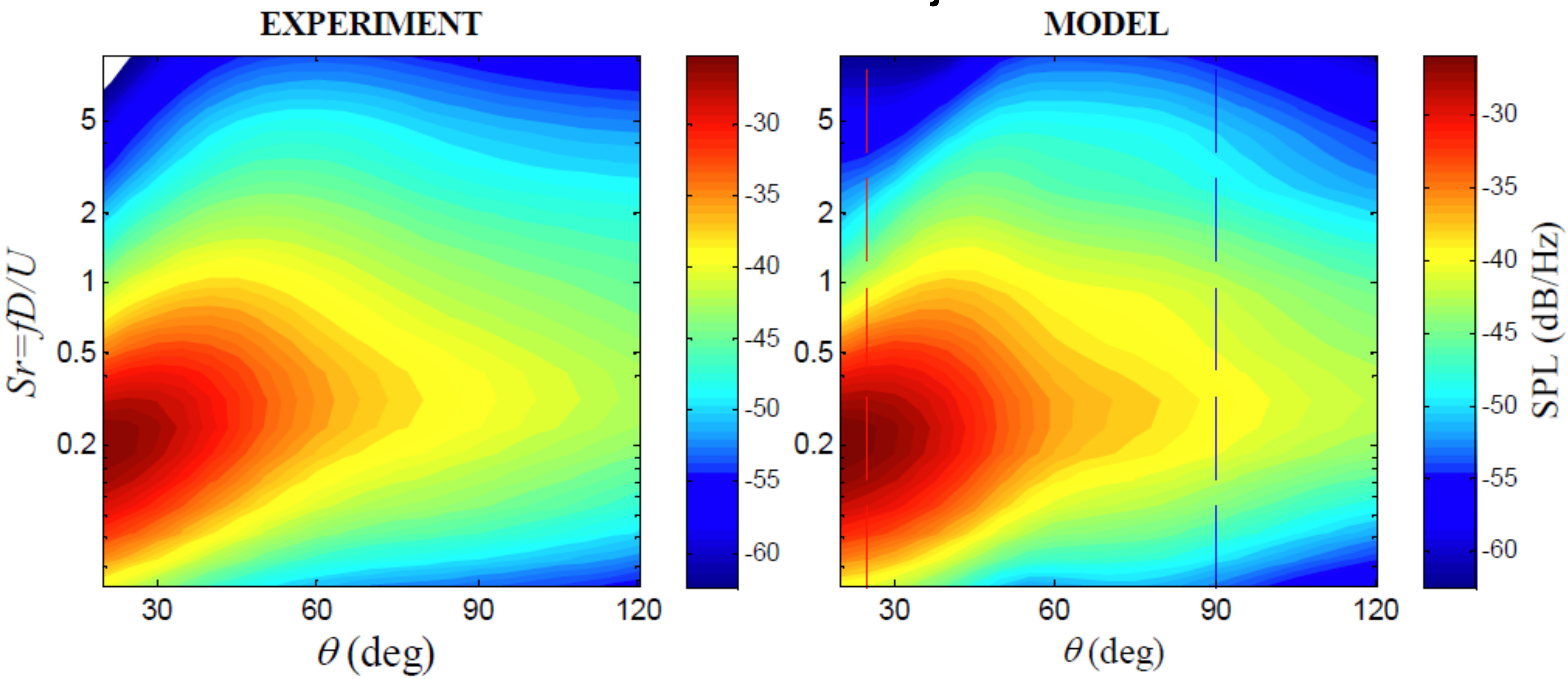

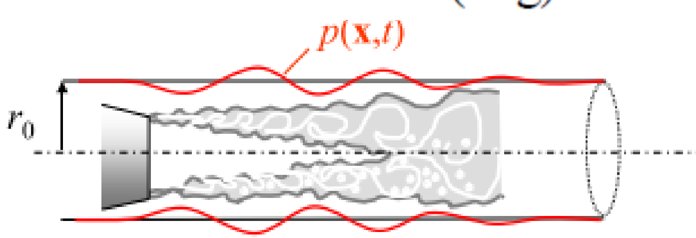

(Papamoschou 2011)

Approach

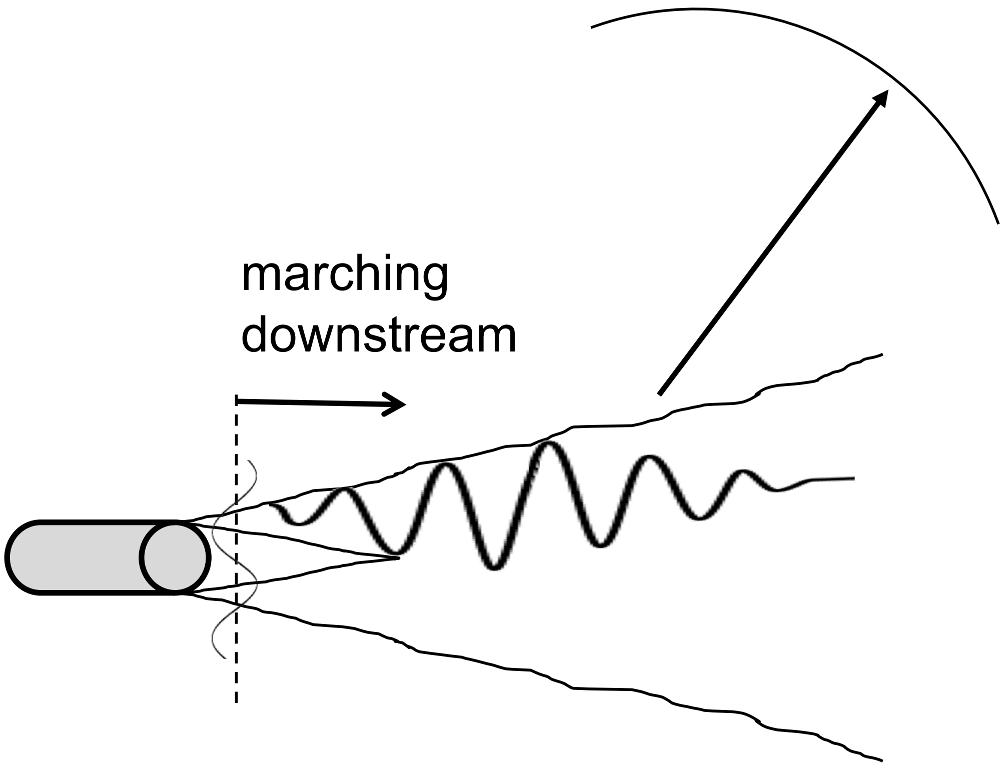

PSE

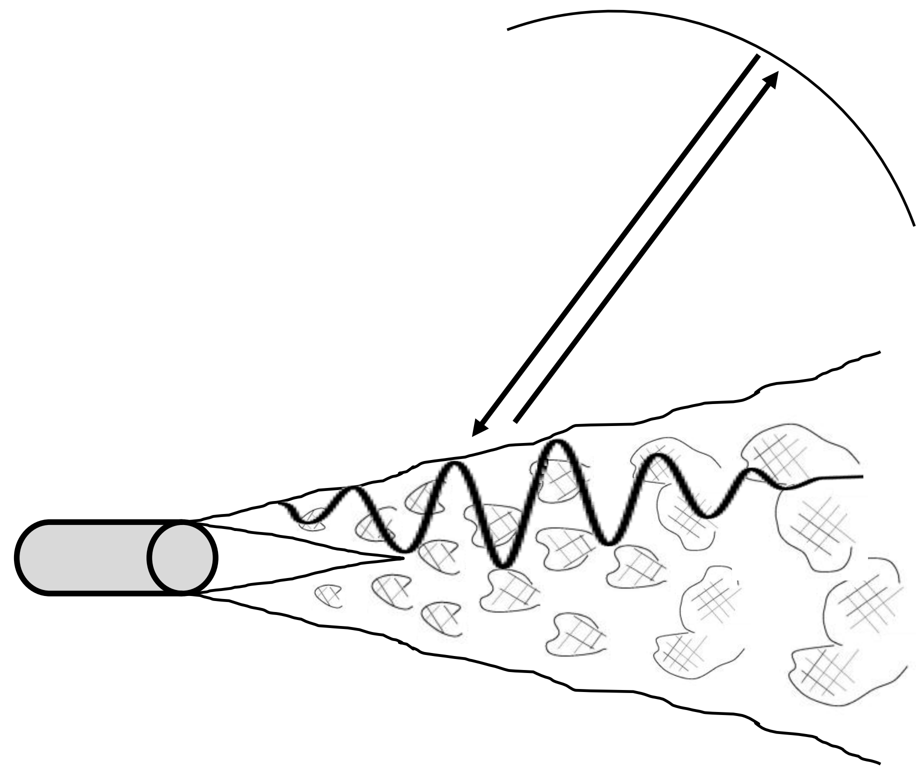

Input-output analysis

Approach: input-output analysis

- Linearized Navier-Stokes equations:

$$\dot{q} = Aq + Bf \leftarrow \textbf{Input}$$

$$\textbf{Output} \leftarrow y = Cq$$

Treat nonlinear terms as forcing driving a linear system

(Same as acoustic analogy)

- Wave-like modal decomposition: $f = \hat{f}e^{i(m\theta-\omega t)}$

$$\hat{y} = \underbrace{C(-i\omega I - A)^{-1}B}_{H}\hat{f}$$

(McKeon & Sharma 2010)

Approach: input-output analysis

- Singular value decomposition (SVD):

$$\boxed{H = U\Sigma V^* \ \text{ or } \ HV = U\Sigma} \quad \text{and} \quad \boxed{\sigma = \frac{\|y\|}{\|f\|} : gain}$$

where $U, V : unitary\ matrices$

$\Sigma : a\ matrix\ whose\ diagonal\ consists\ of\ \sigma's$

→ How each column of V (input vector) is mapped to the corresponding column of U (output vector) through H

- SVD of H computed through eigen-decomposition of H^+H

$$\boxed{H^+H = B^+(z^*I - A^+)^{-1}C^+C(zI - A)^{-1}B}$$

where $()^* : complex - conjuate\ transpose$

$()^+ : adjoint\ operator$

Base flows

- Reynolds-Averaged Navier-Stokes (RANS) solutions
  - Ideally expanded, axisymmetric, isothermal turbulent jets
  - Modified $k{-}\varepsilon$ turbulence model (Thies & Tam 1995)
  - $M_j = \frac{u_j}{c_j} = 0.9$ jet at $Re_D = 2{\times}10^5$

Contours of axial velocity normalized by the nozzle exit velocity for a M_j = 0.9 jet

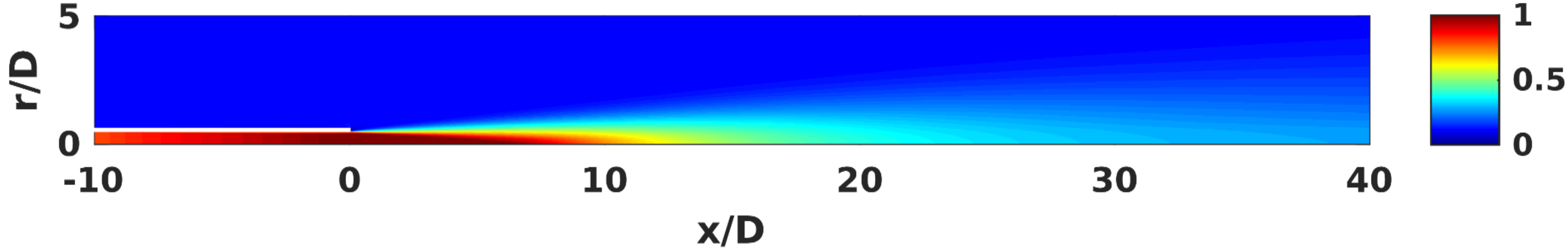

(Full domain: -10 < x/D < 40, 0 < r/D < 25)

Input-output analysis

- Matrices B and C define input & output domains

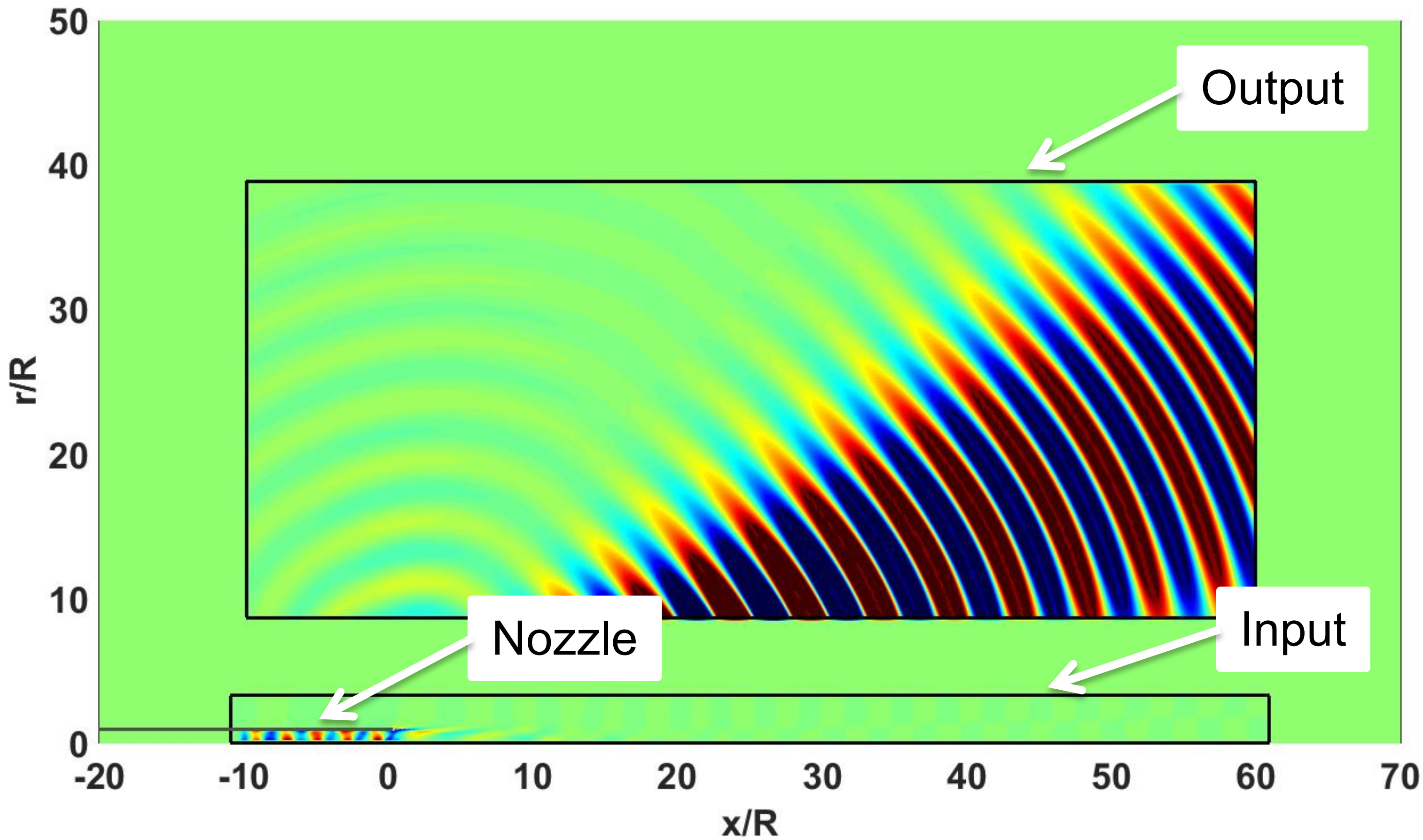

Acoustic response (supersonic)

Output modes

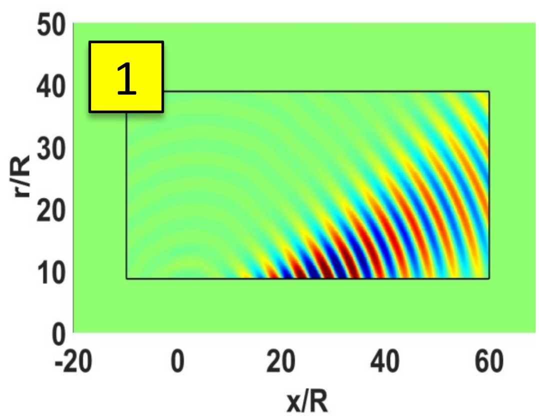

M_j = 1.5 isothermal jet (m=0)

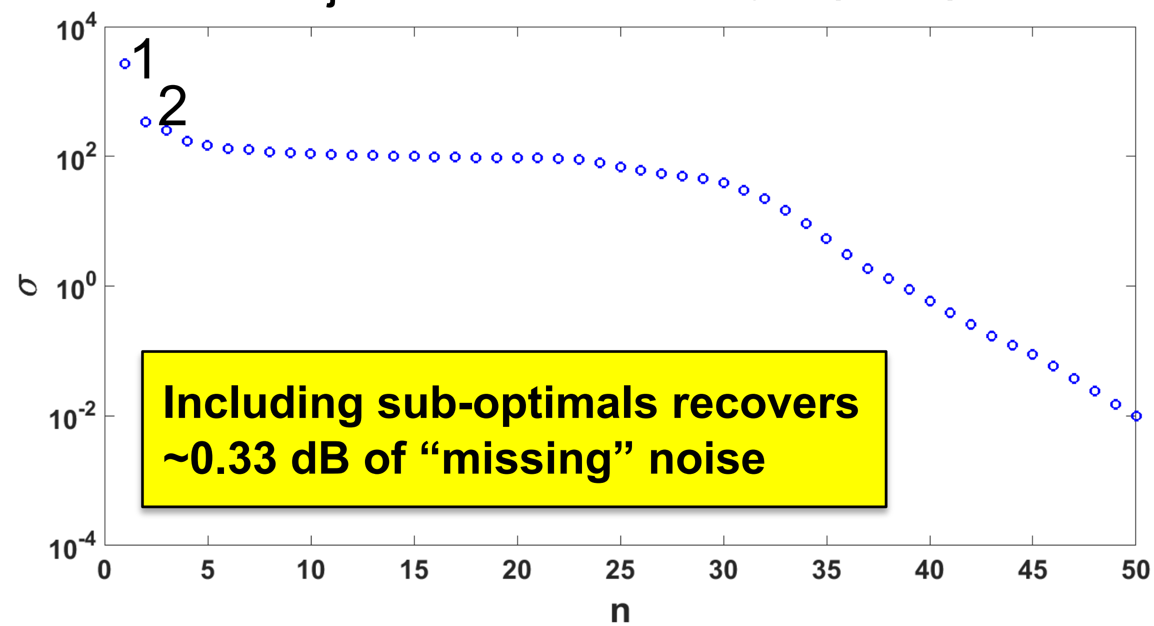

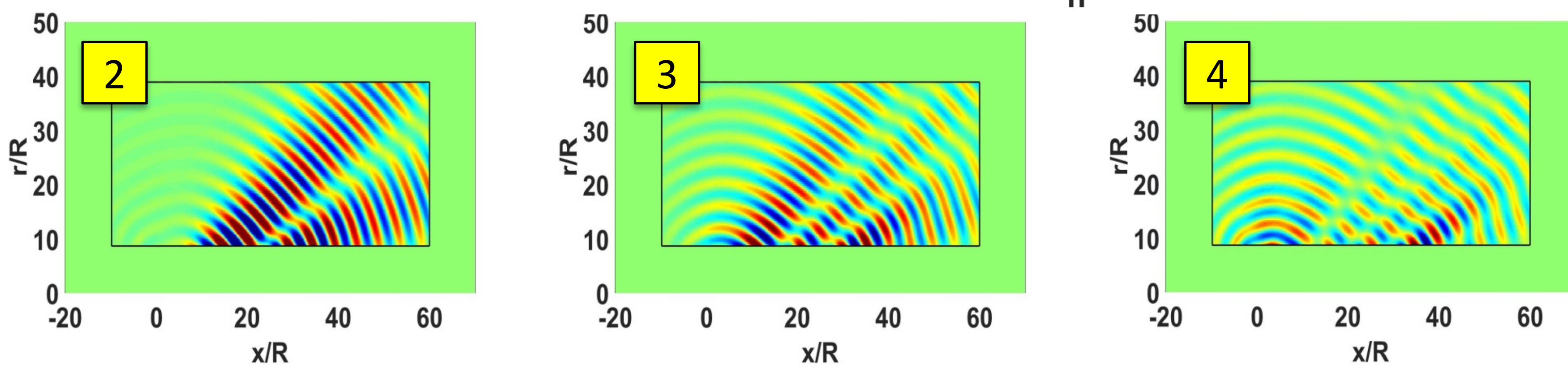

(Jeun, Nichols, & Jovanovic, PoF 2016; AIAA Paper 2016; AIAA Paper 2017)

Input modes

M_j = 1.5 isothermal jet (m=0)

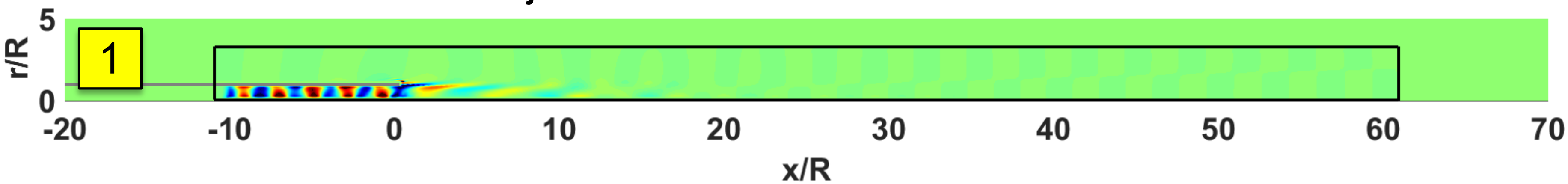

M_j = 0.9 isothermal jet (m=0)

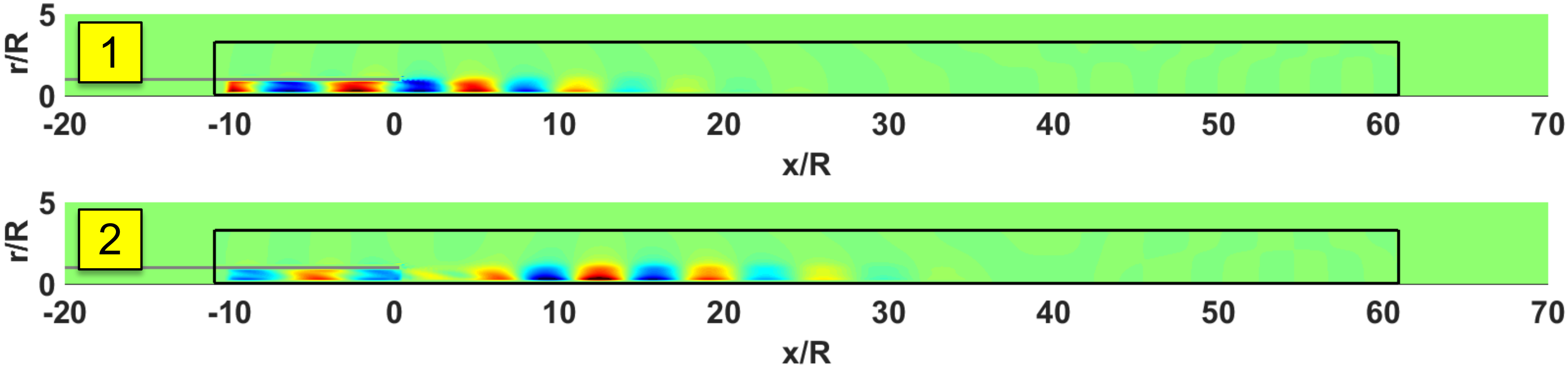

(Jeun, Nichols, & Jovanovic, PoF 2016; AIAA Paper 2016; AIAA Paper 2017)

Reconstructed acoustic field

High fidelity simulations

Optimal mode alone (PSE)

24 modes

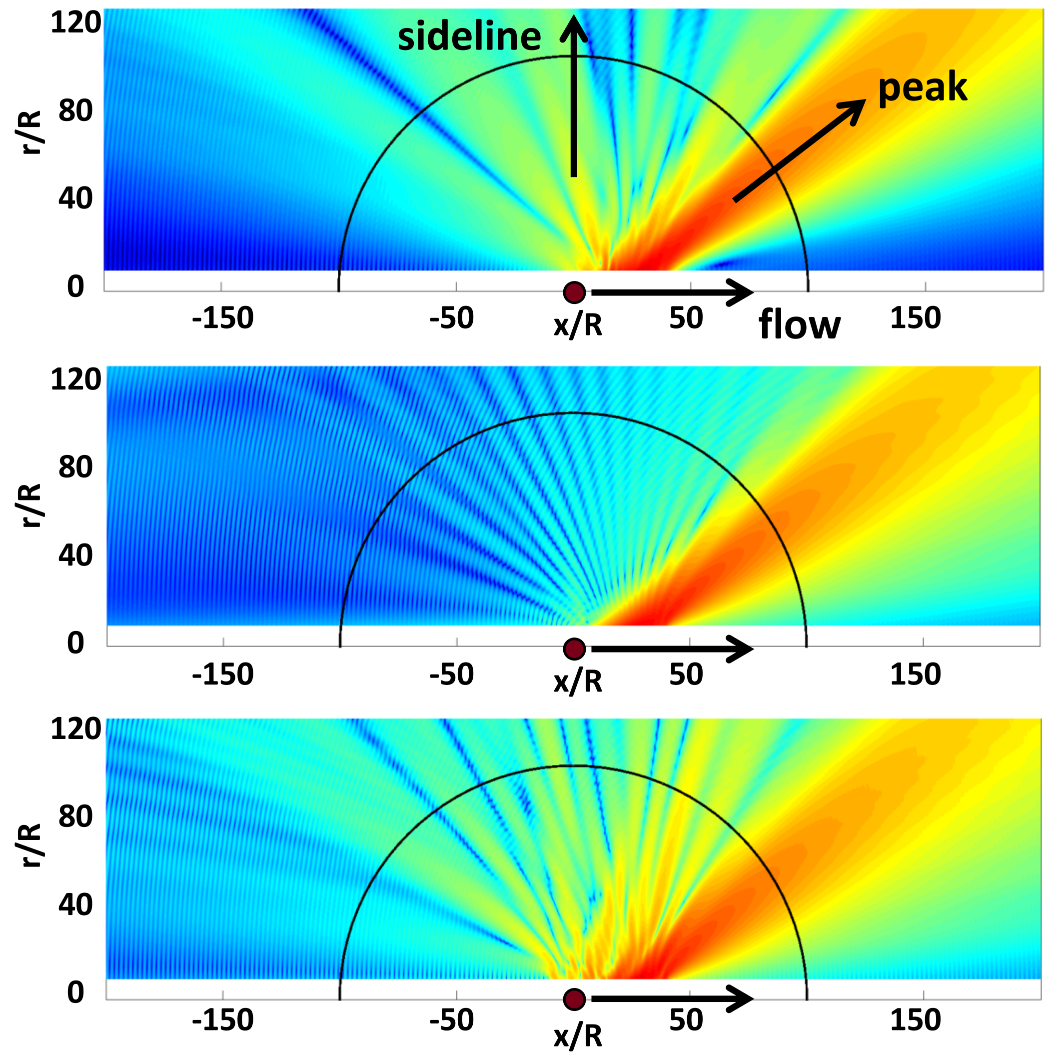

(Jeun, Nichols, & Jovanovic, PoF 2016; AIAA Paper 2016; AIAA Paper 2017)

Realistic input forcings

- Allow forcings only where TKE is active
- B matrix weights inputs by TKE

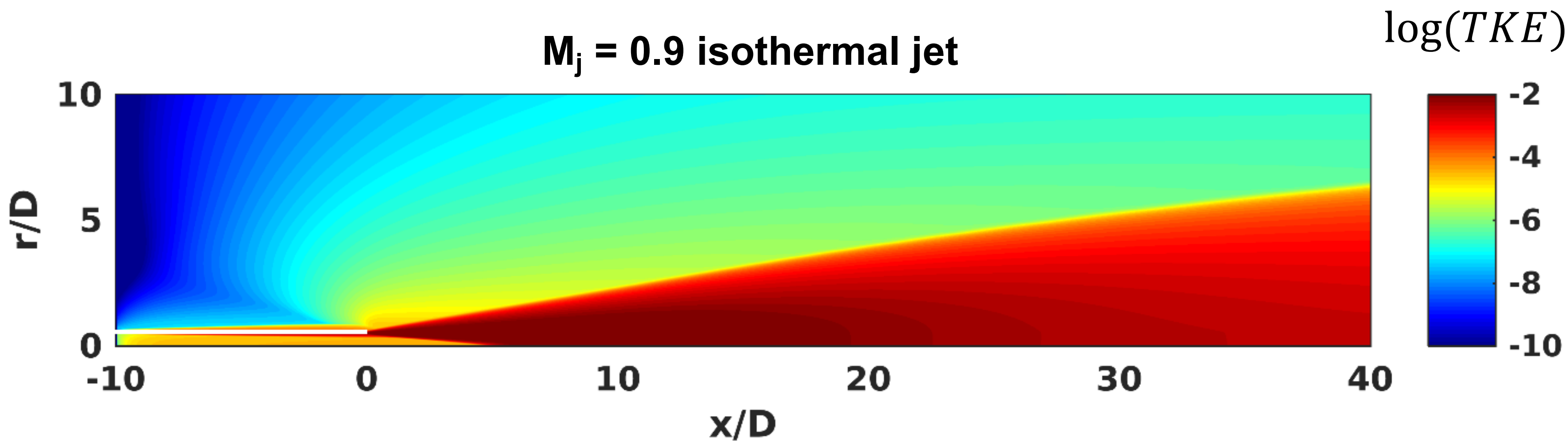

(Jeun & Nichols, arXiv:1806.09280, 2018)

Outputs of interest

- C matrix specifies far-field observers distributed uniformly along an arc at a distance of 100 diameters from the nozzle exit

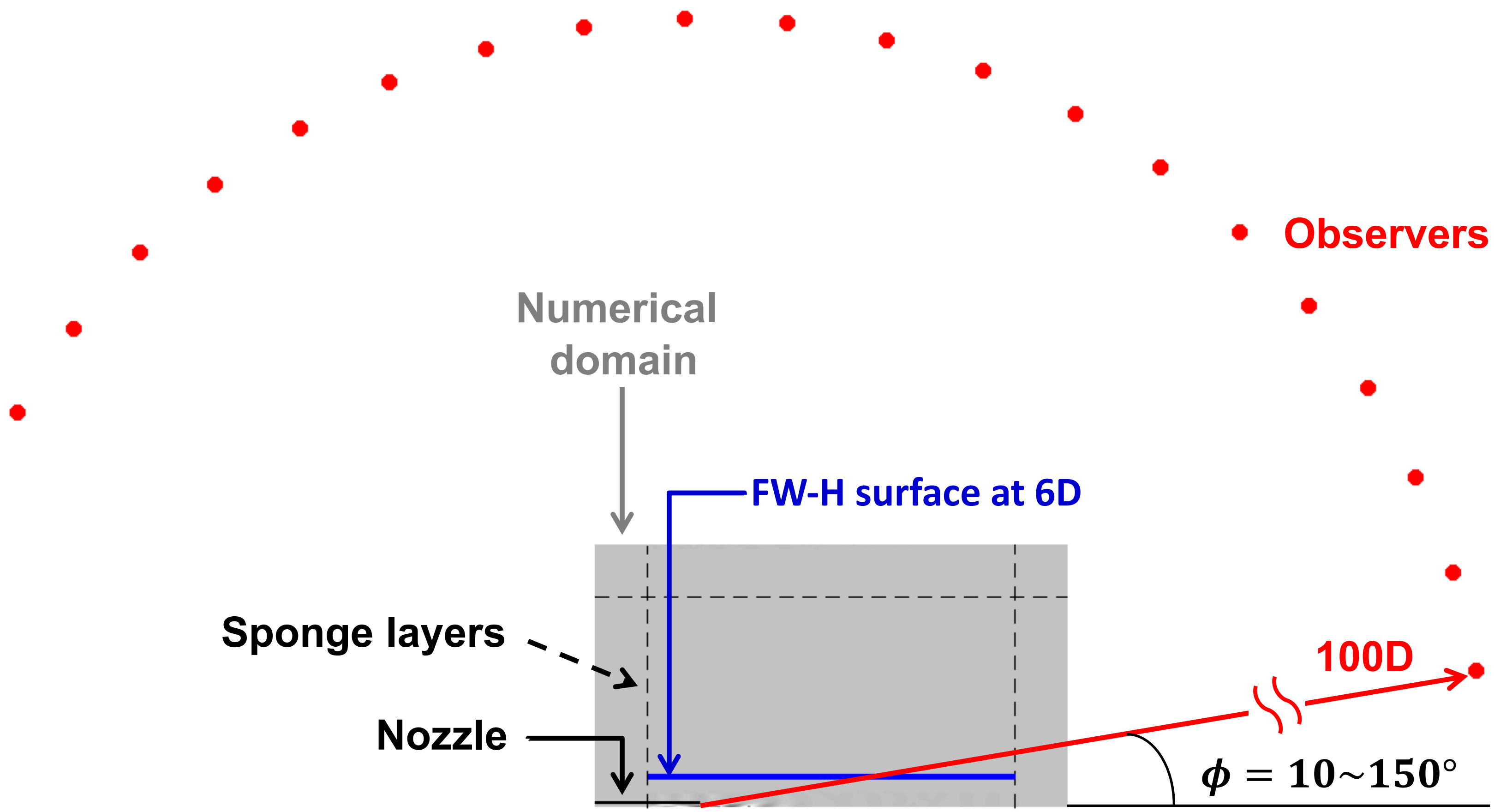

(Jeun & Nichols, AIAA Paper 2017; 2018)

M_j = 0.9 isothermal jet (m=0)

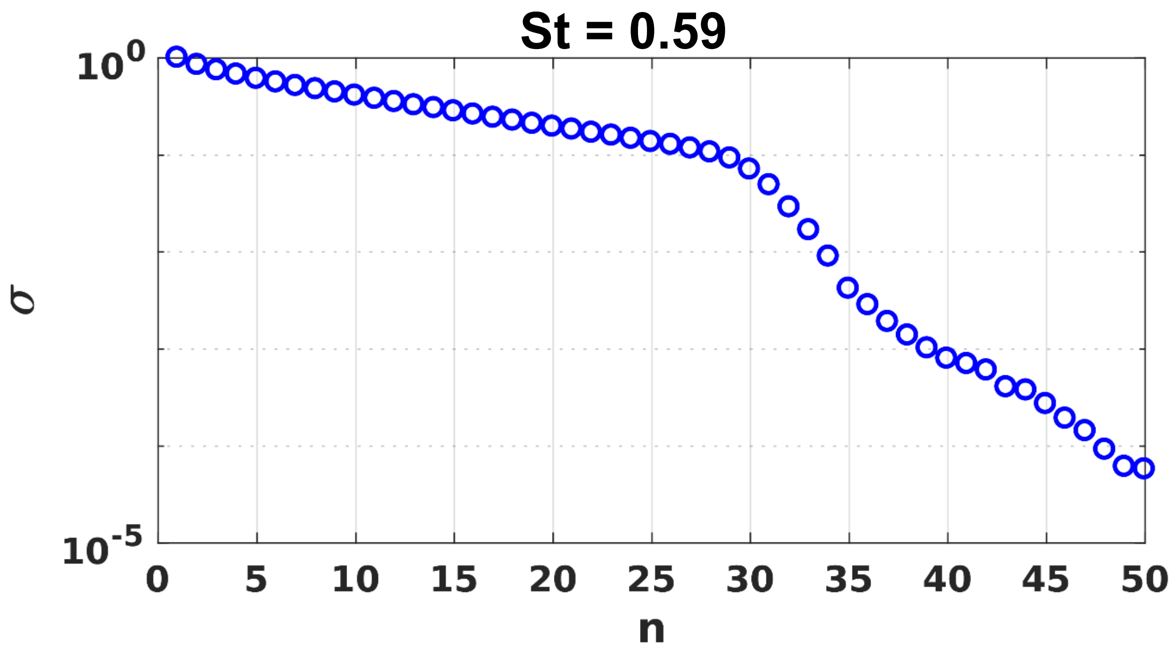

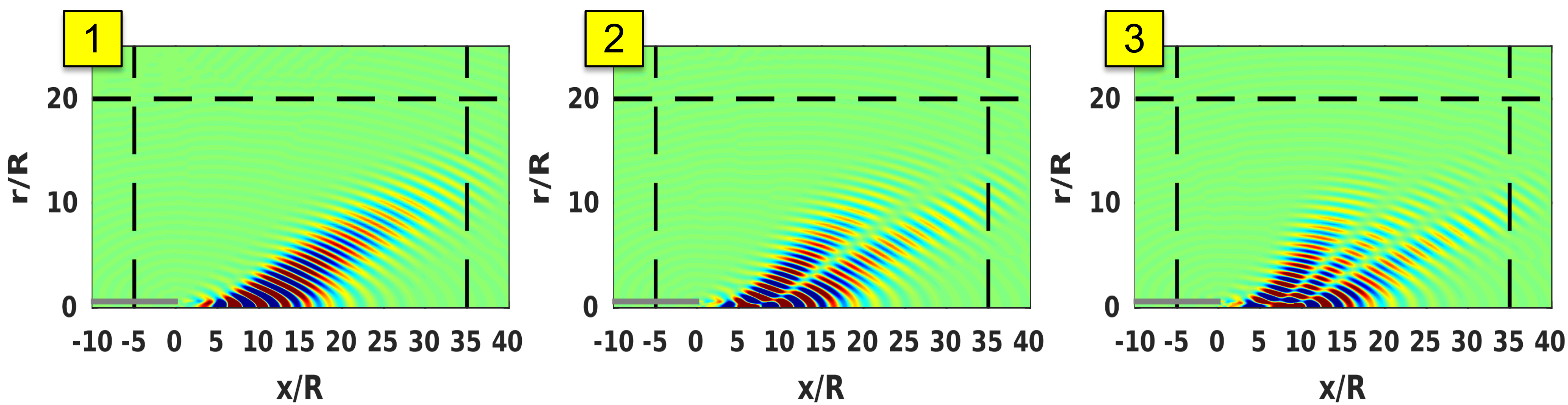

M_j = 0.9 isothermal jet (m=0)

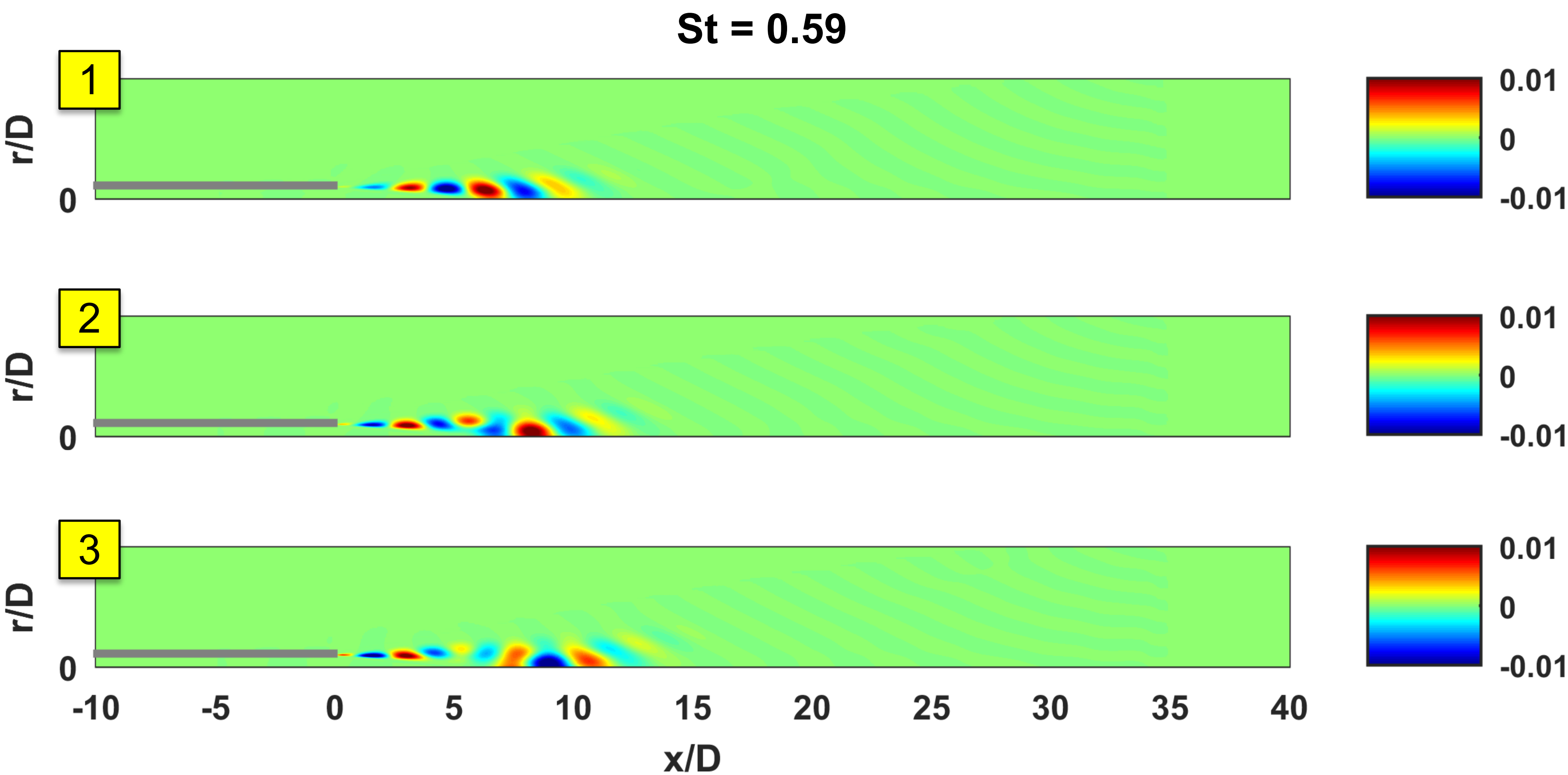

(Jeun & Nichols, arXiv:1806.09280, 2018)

Optimal acoustic source

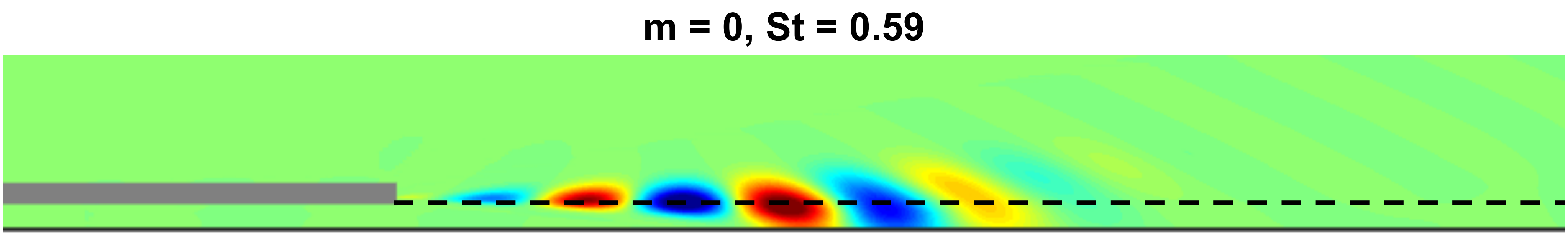

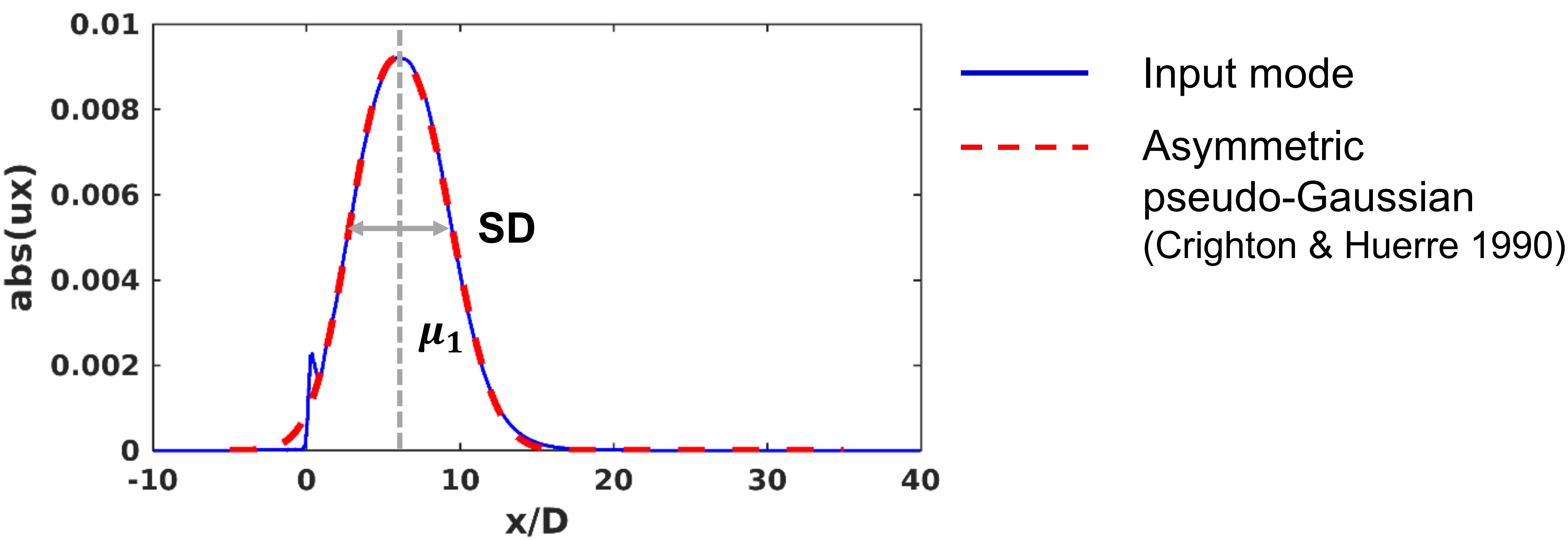

Similarity wavepackets

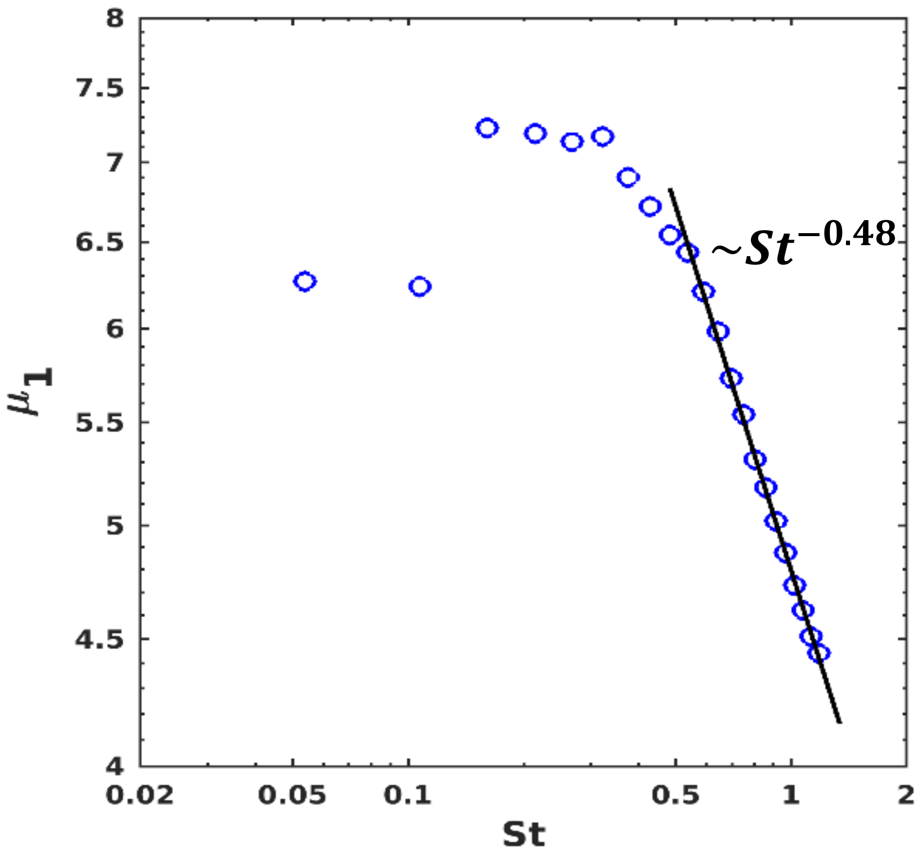

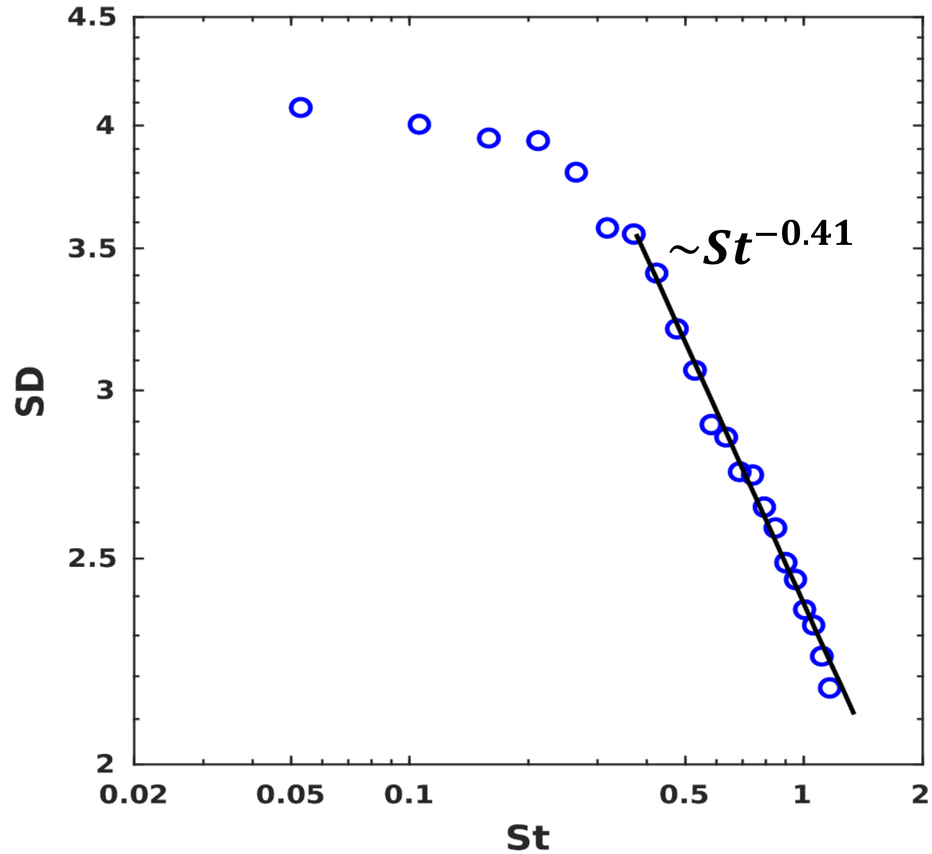

→ Optimal wavepacket is similar over frequencies (St > 0.5)

Similarity wavepackets

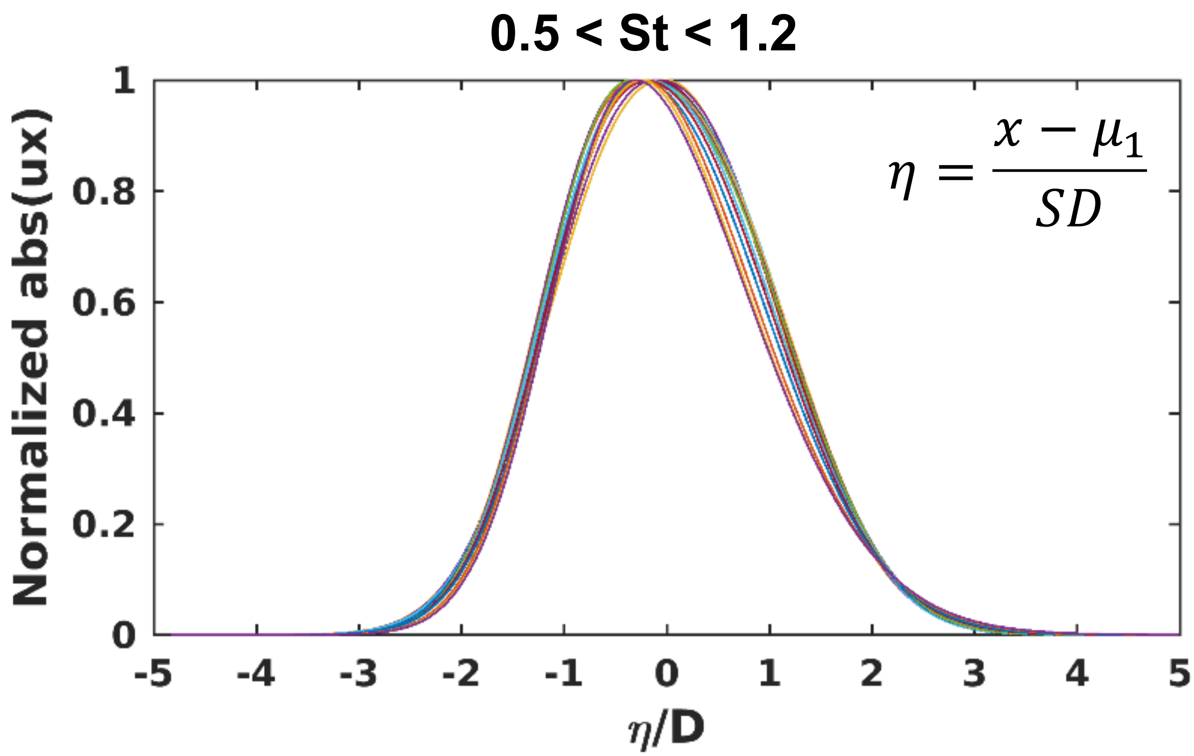

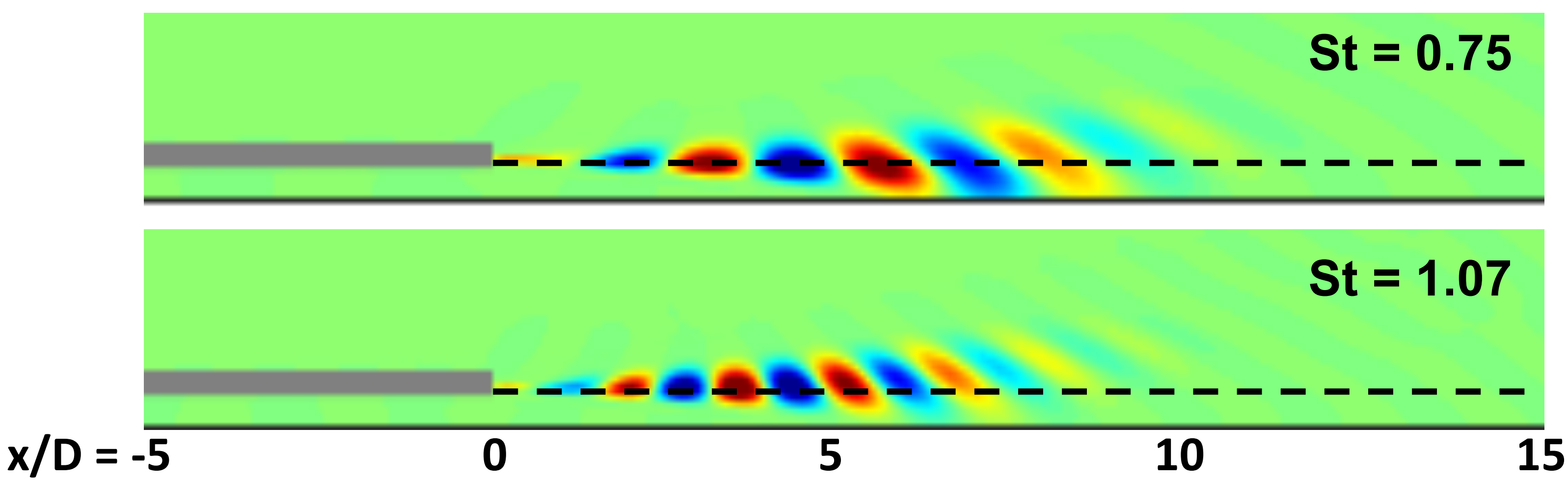

Sub-optimal modes

- Wavepackets embedded in a soup of turbulent fluctuations
- They may not maintain coherence over large distances
- Instead, “pieces” of the wavepacket appear intermittently

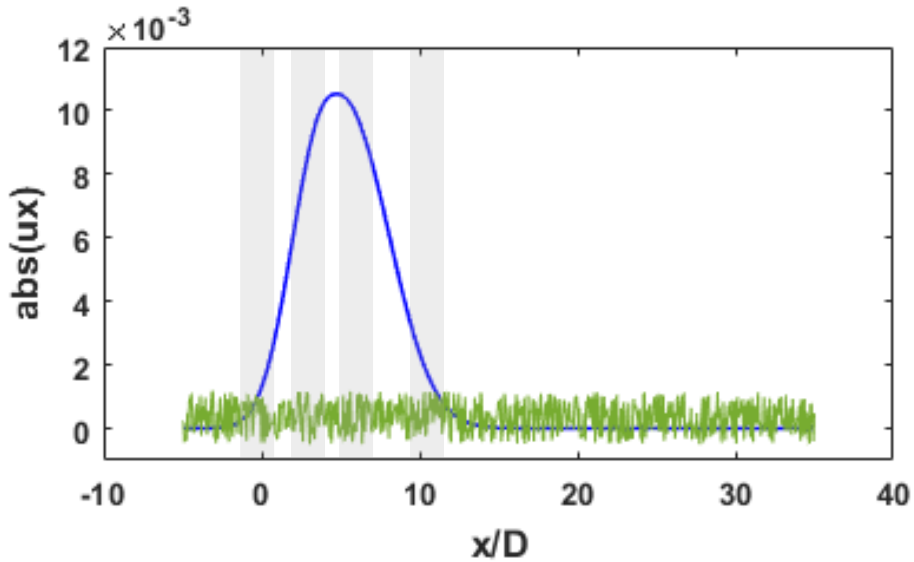

- To model this, we form a matrix whose columns are windows of the wavepacket
  - → Does SVD of this matrix reproduce sub-optimal modes?

Sub-optimal modes

n = 2

n = 3

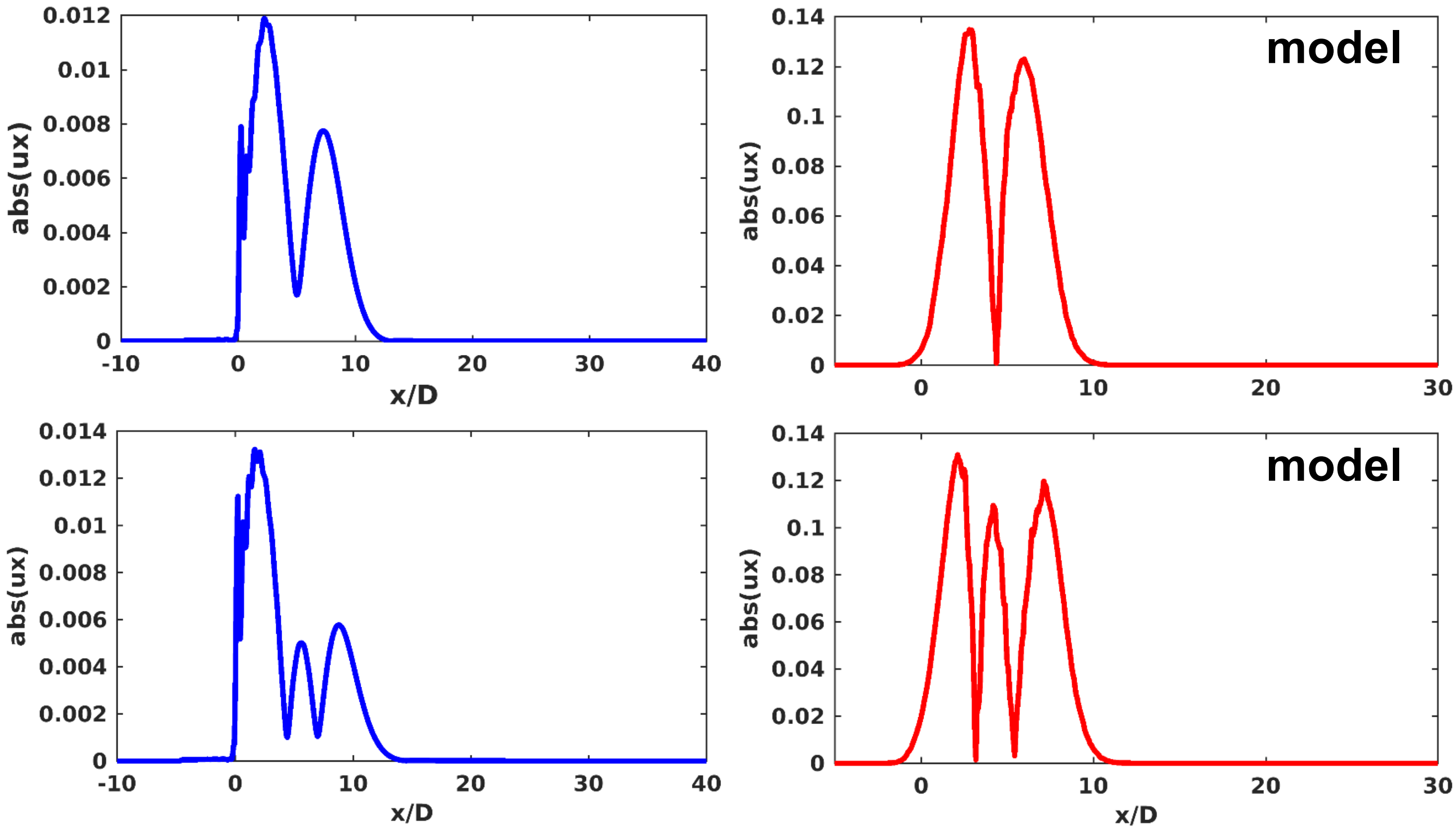

→ Sub-optimal modes represent decoherence of the optimal forcing

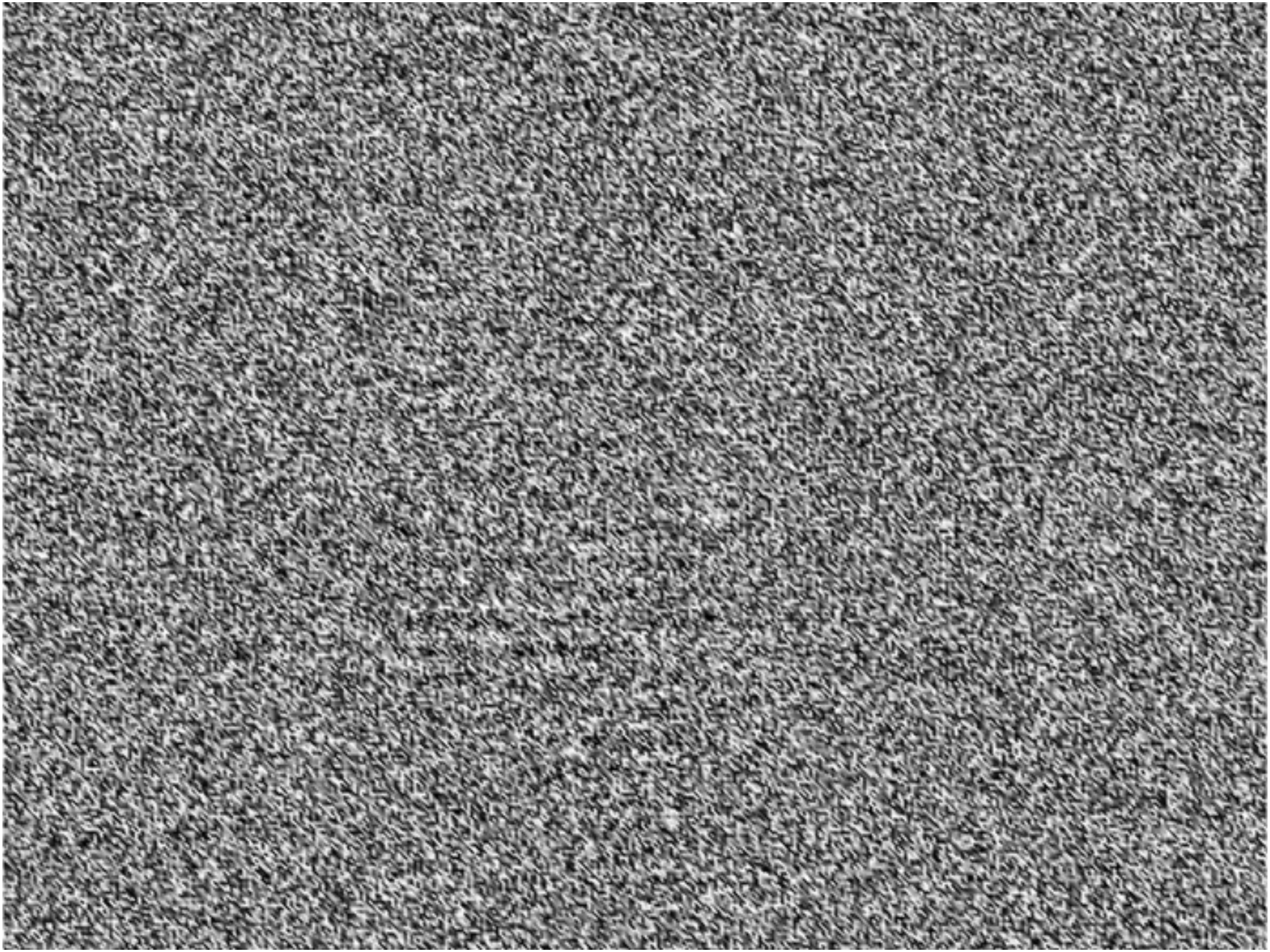

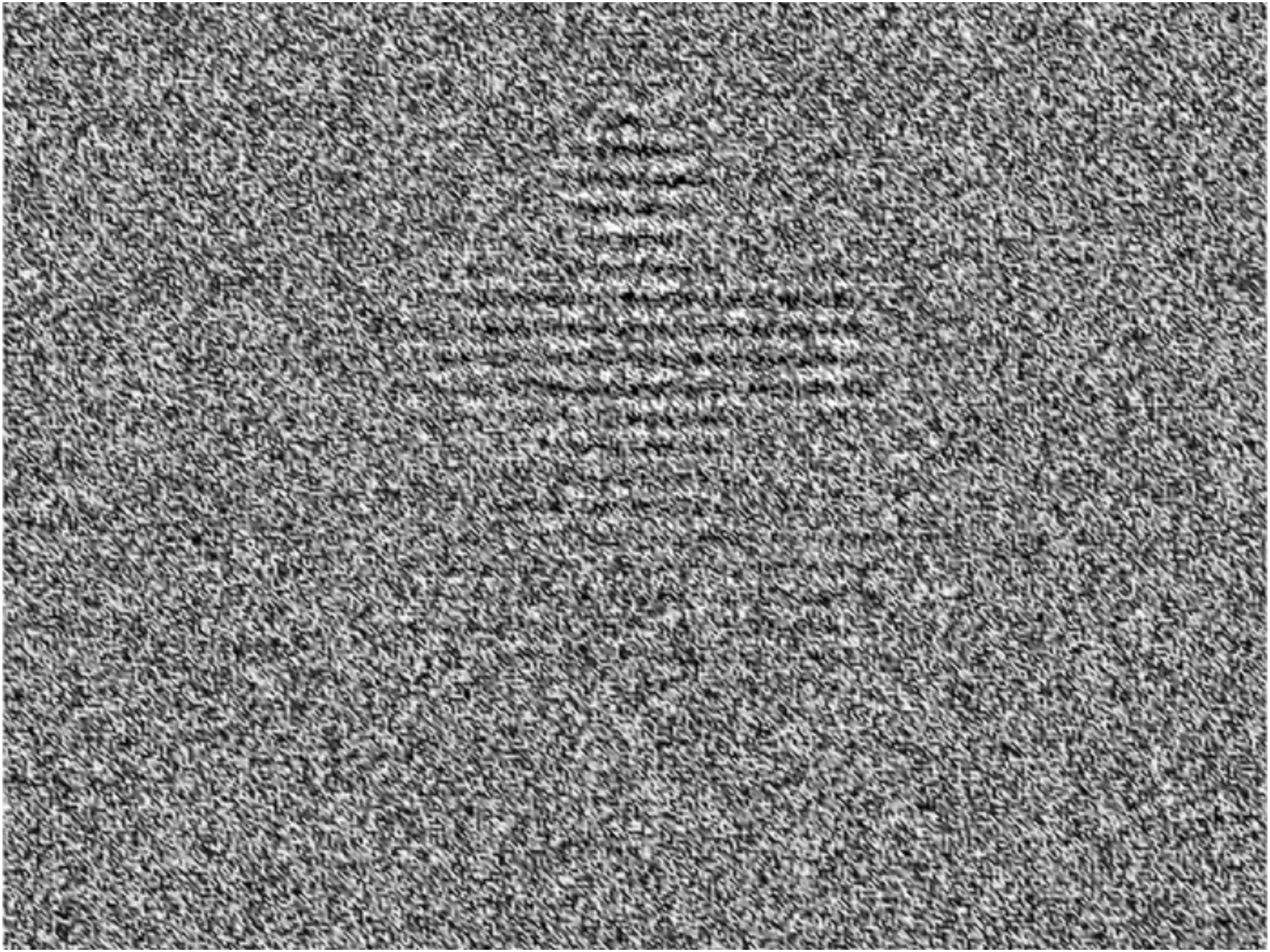

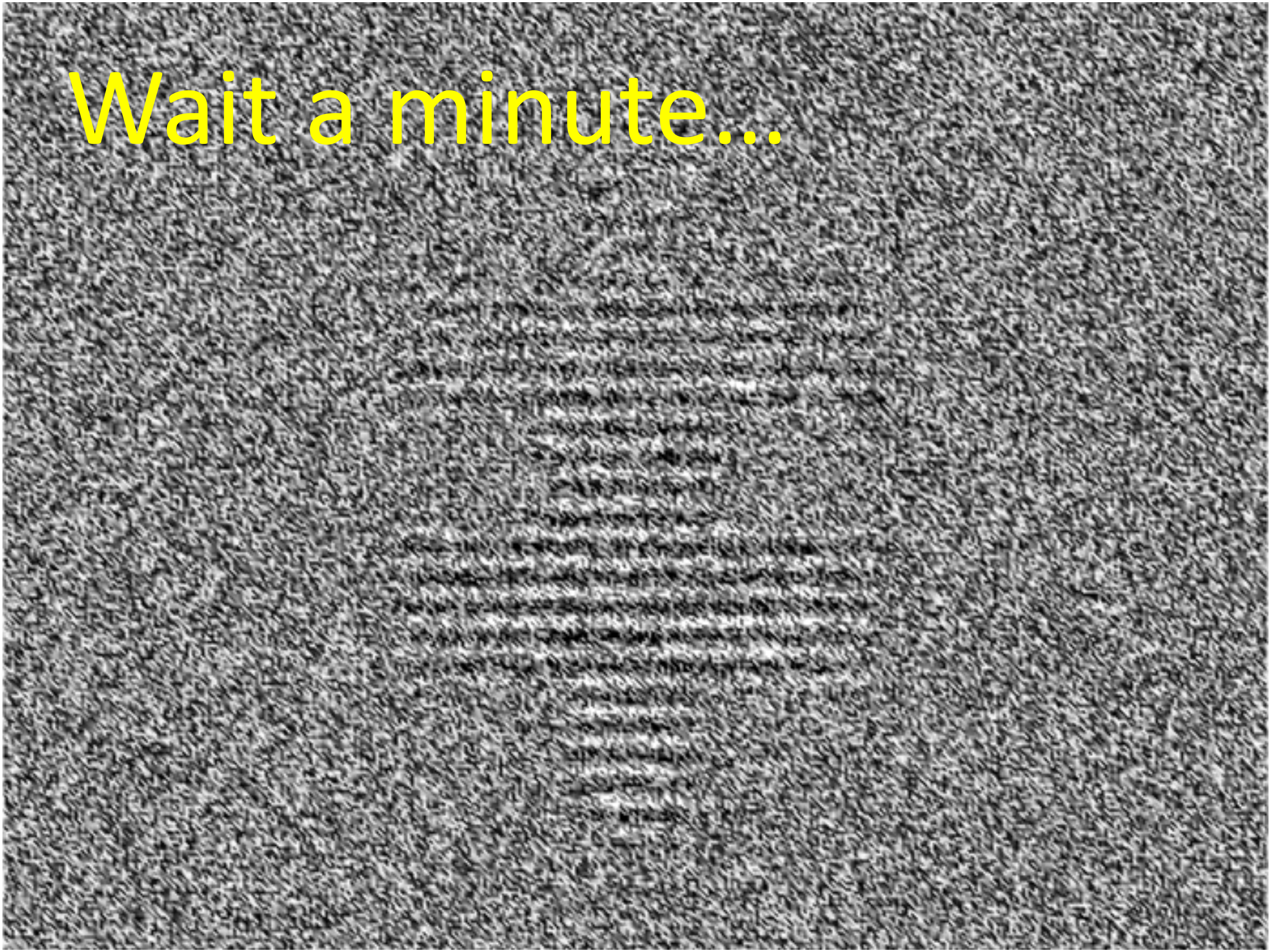
Wait a minute...

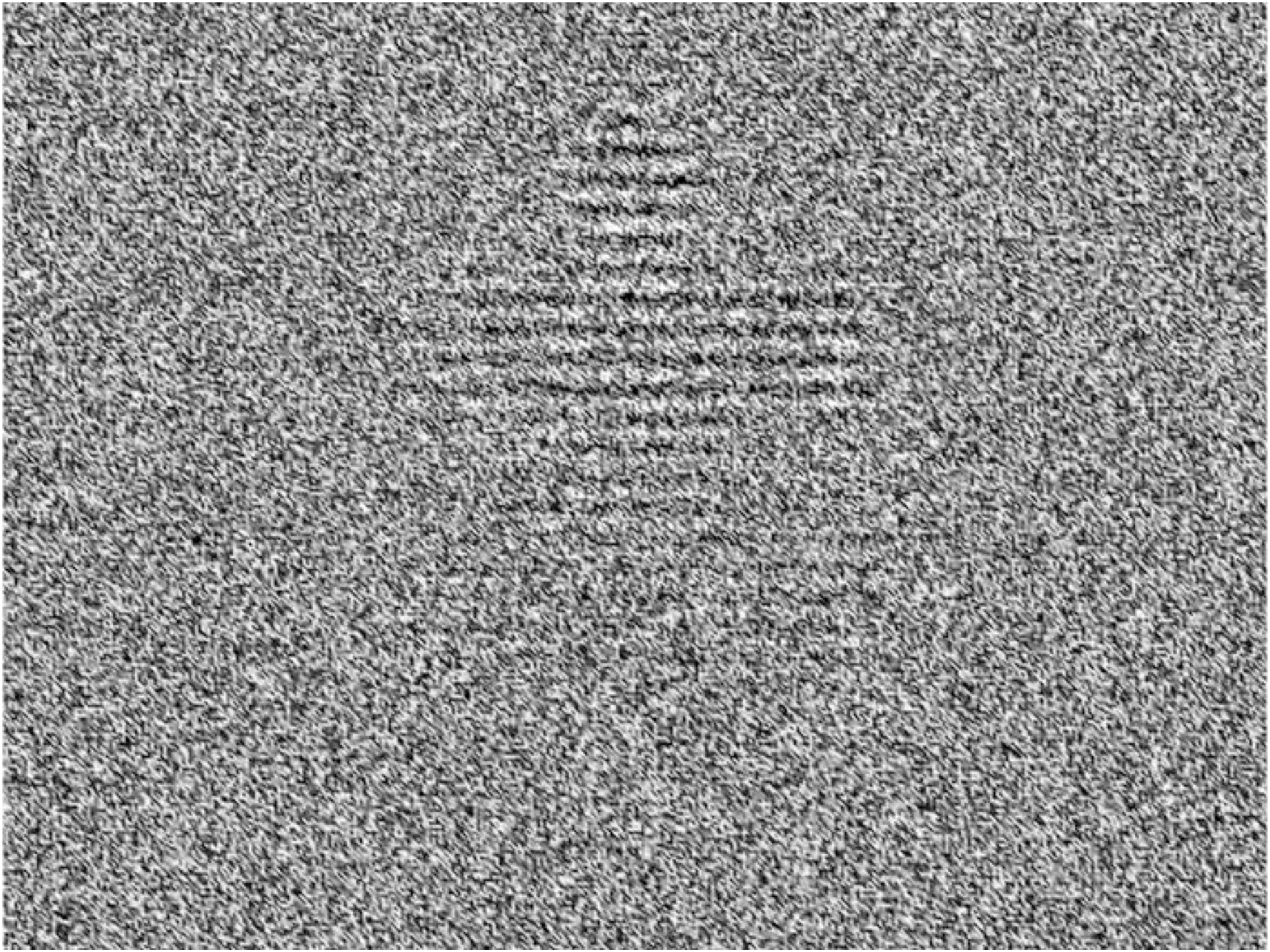

The optimal mode

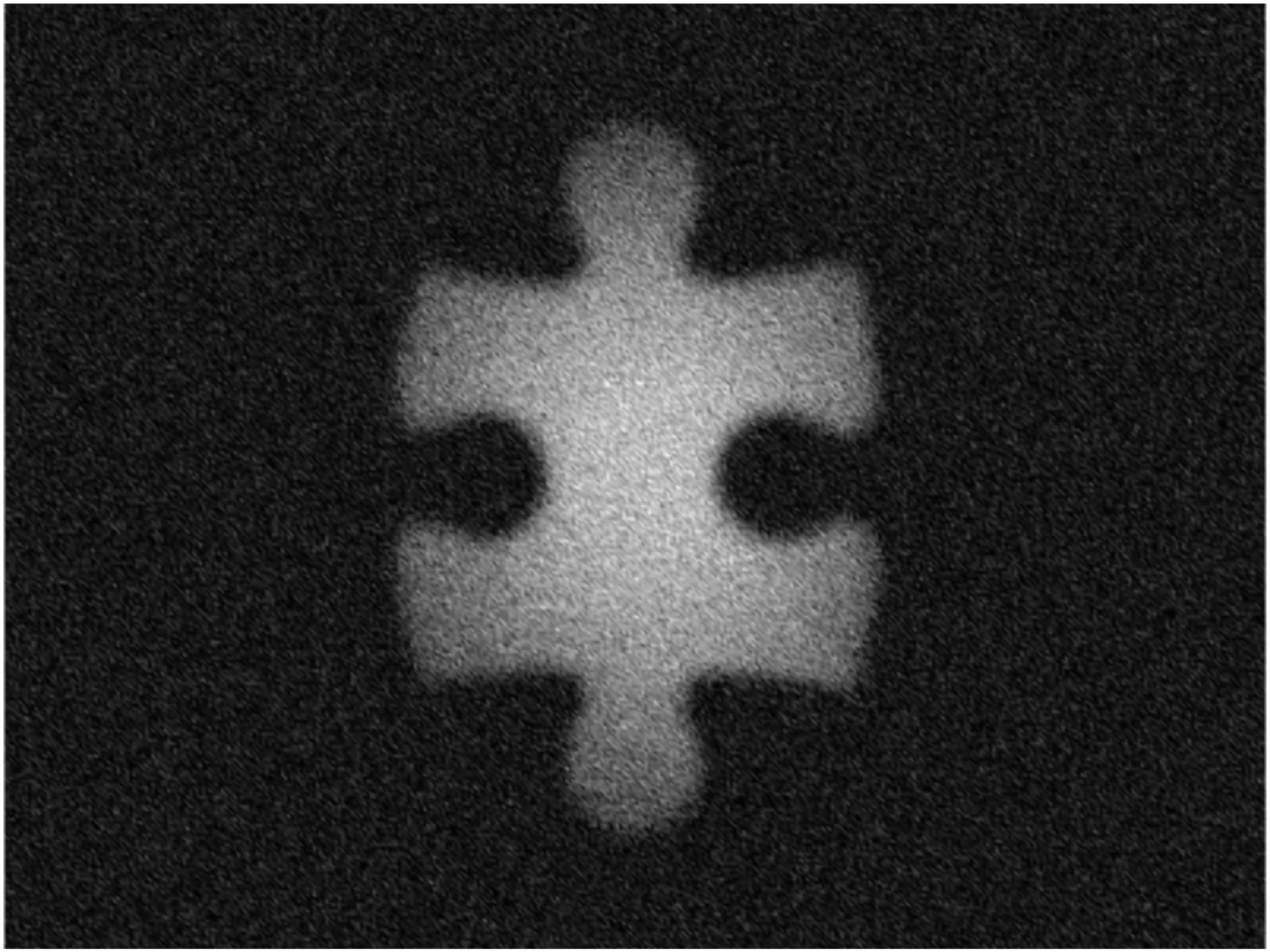

Sub-optimal modes

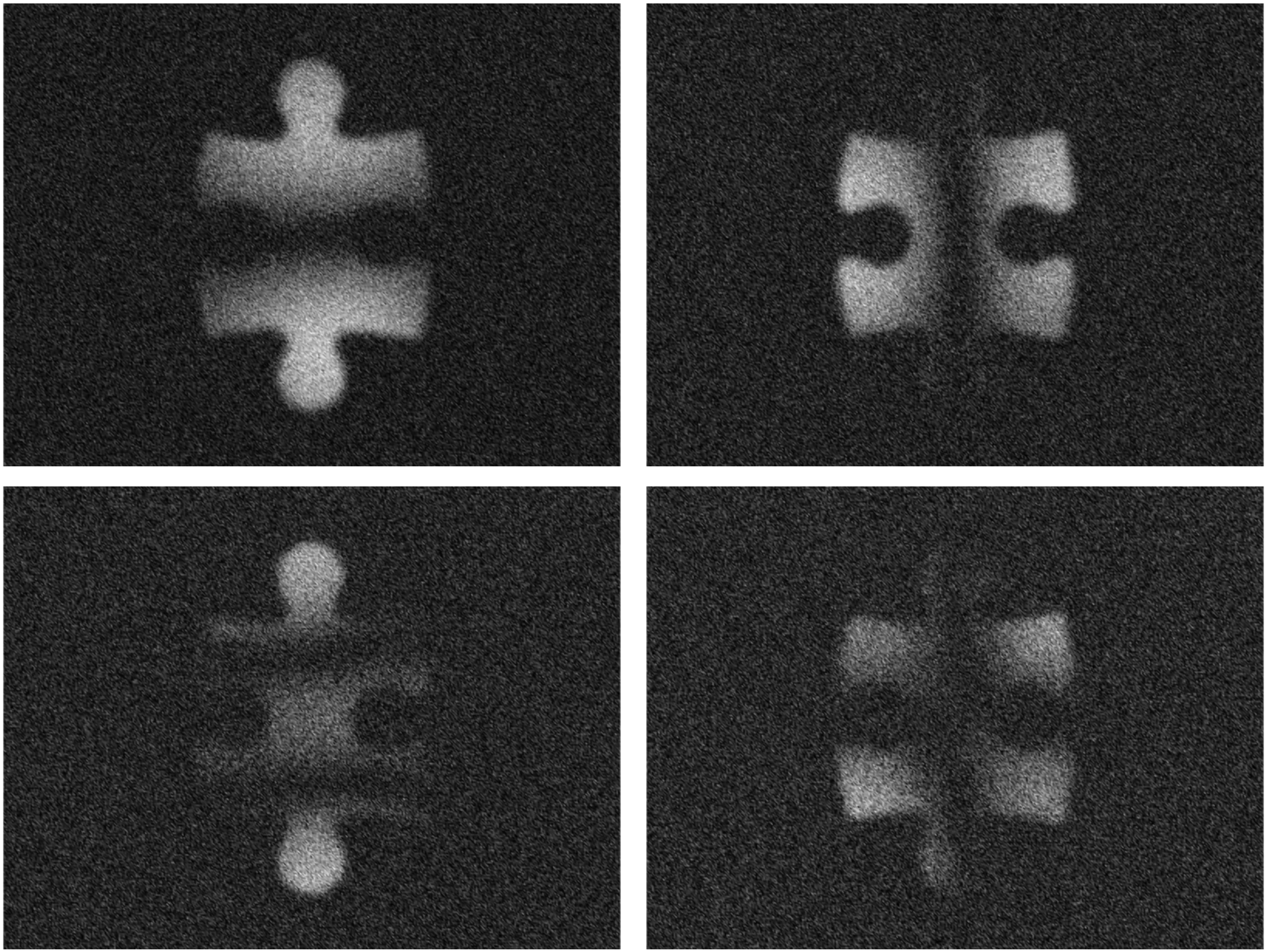

LES for M_j = 0.9 isothermal jet

$Re = 2{\times}10^5$
50M cells, $tc/D = 414$

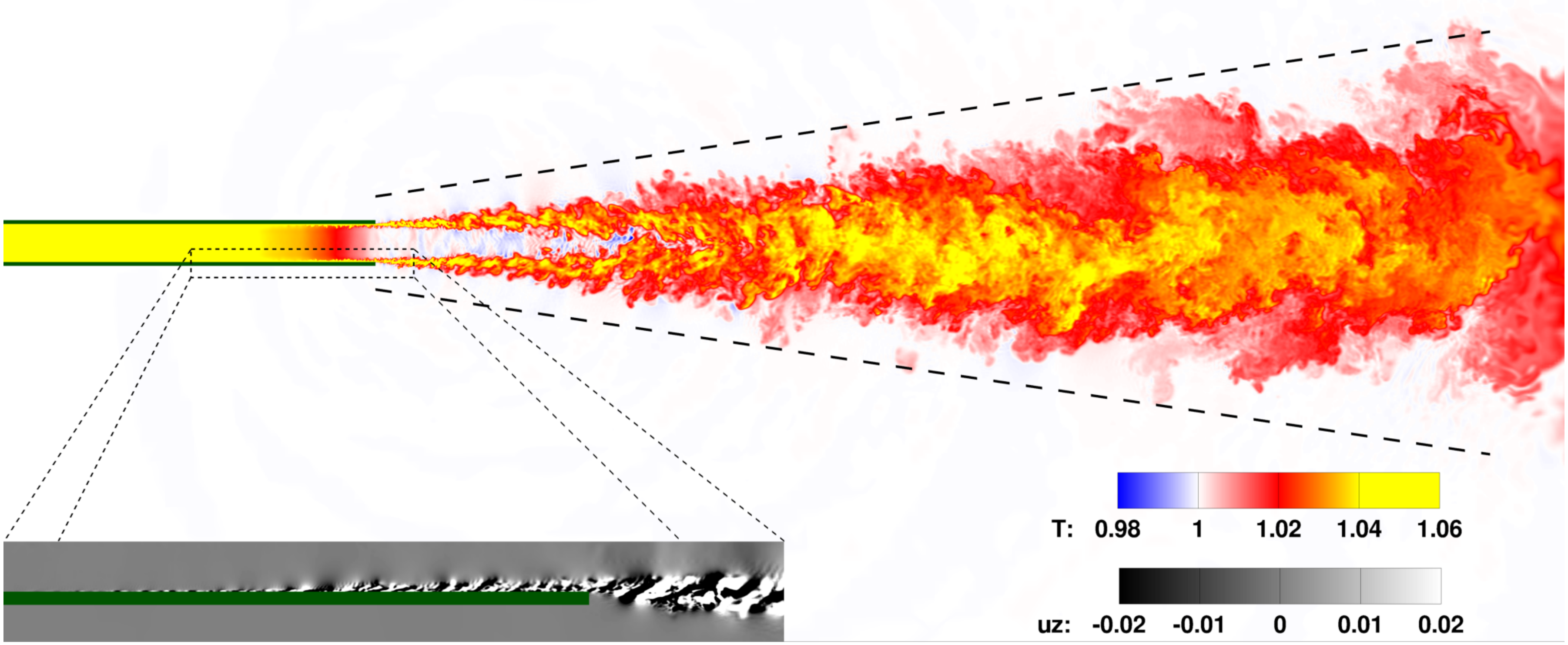

Far-field spectra

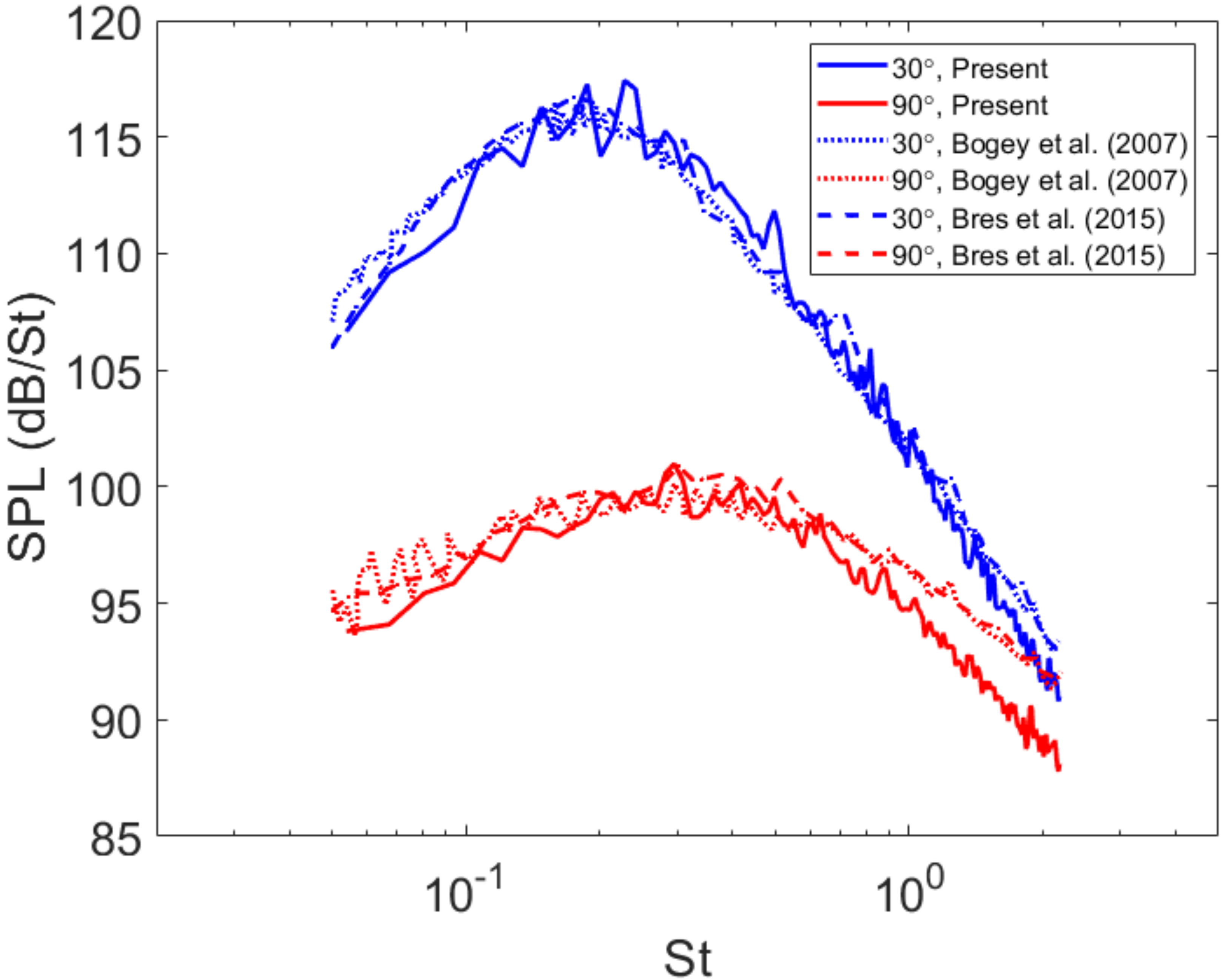

Input projection (St = 0.59)

Reynolds stress from LES, SPOD (Towne et al. 2018)

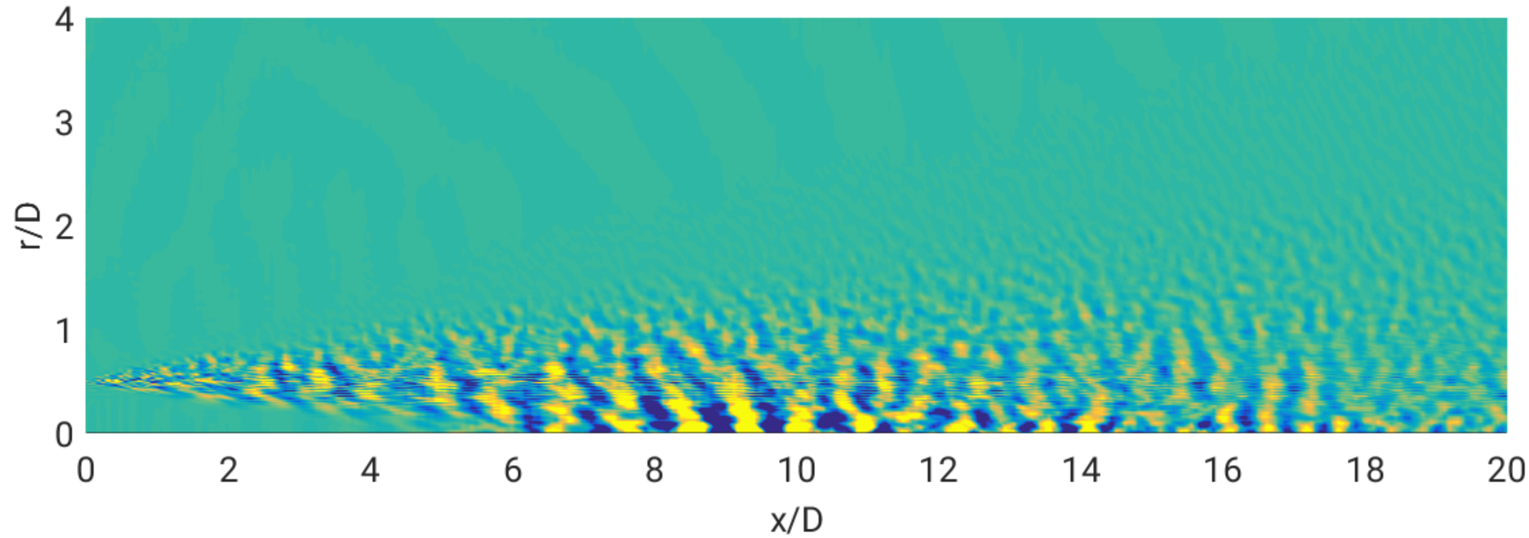

Optimal input forcing

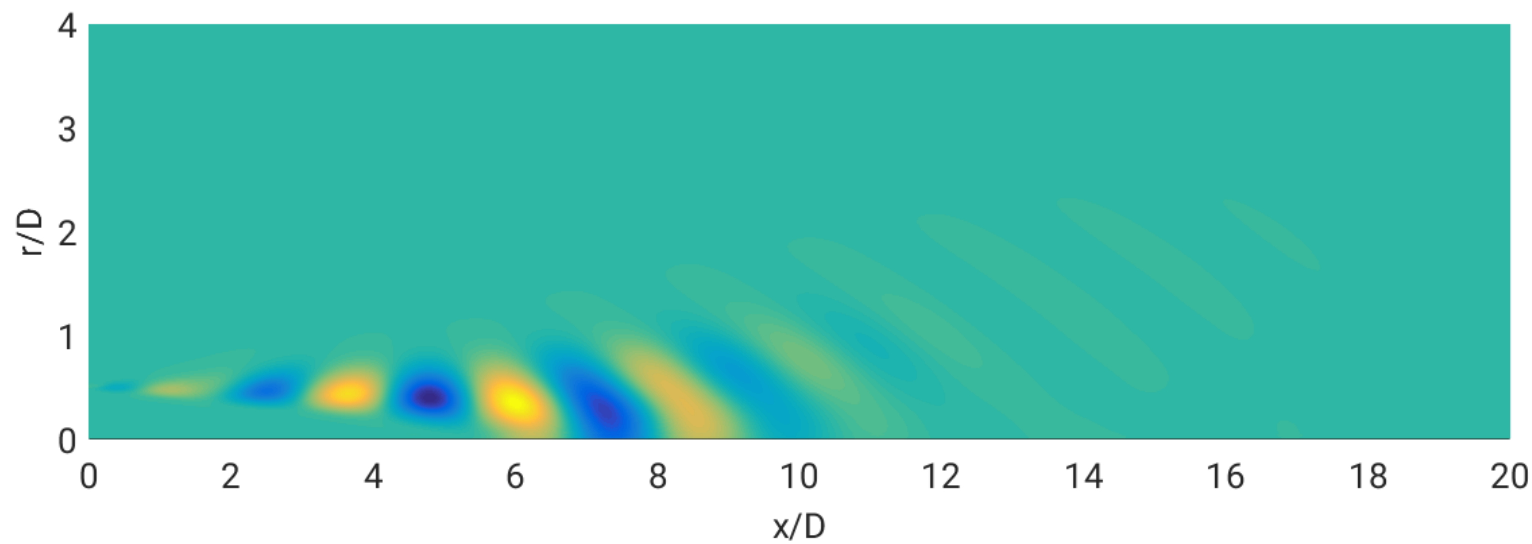

Spatial spectral content

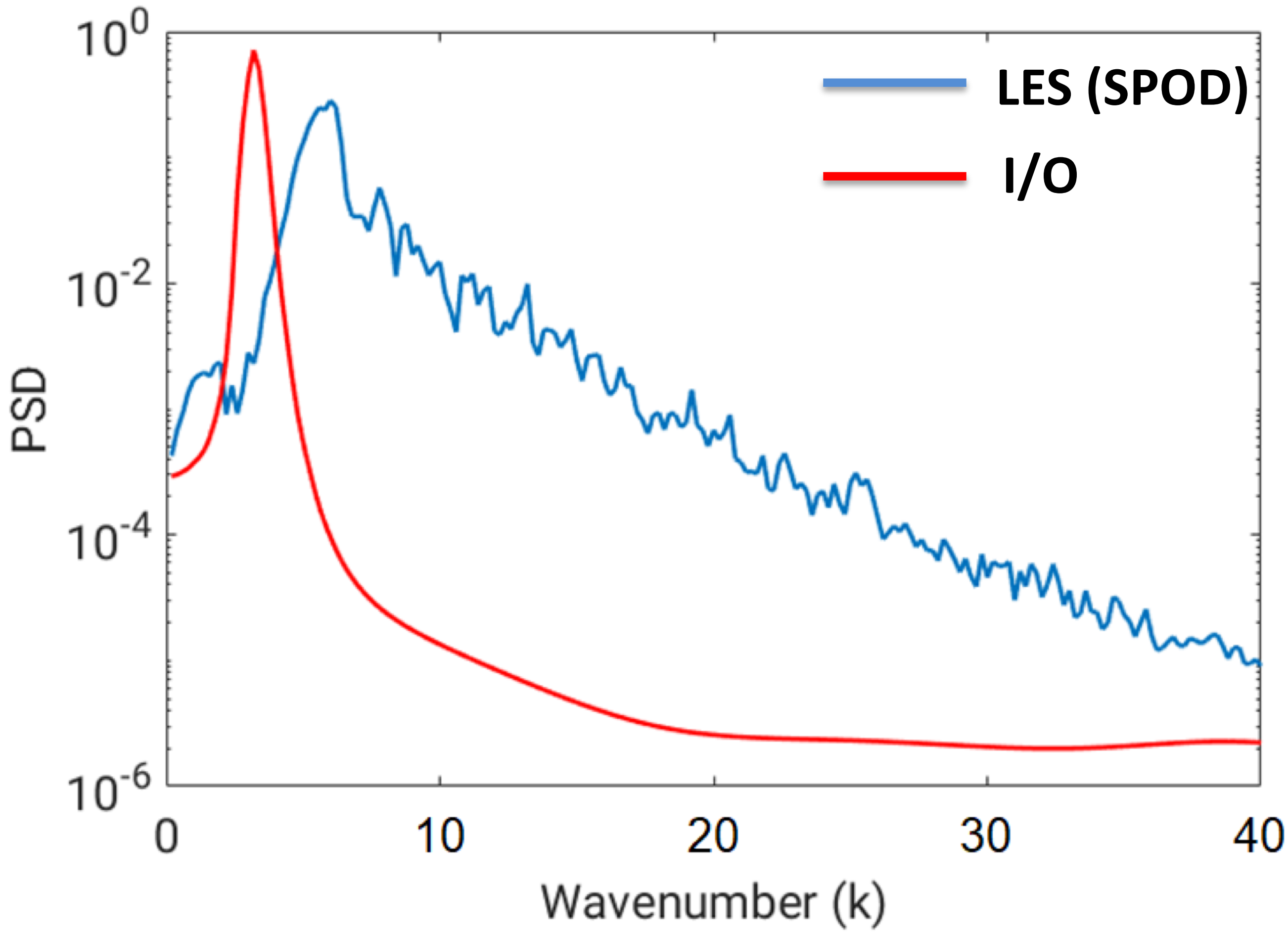

- I/O wavenumber is exactly half that of K-H instability
  - associated with radiating supersonic tail of wavepacket

Spatially subharmonic jitter

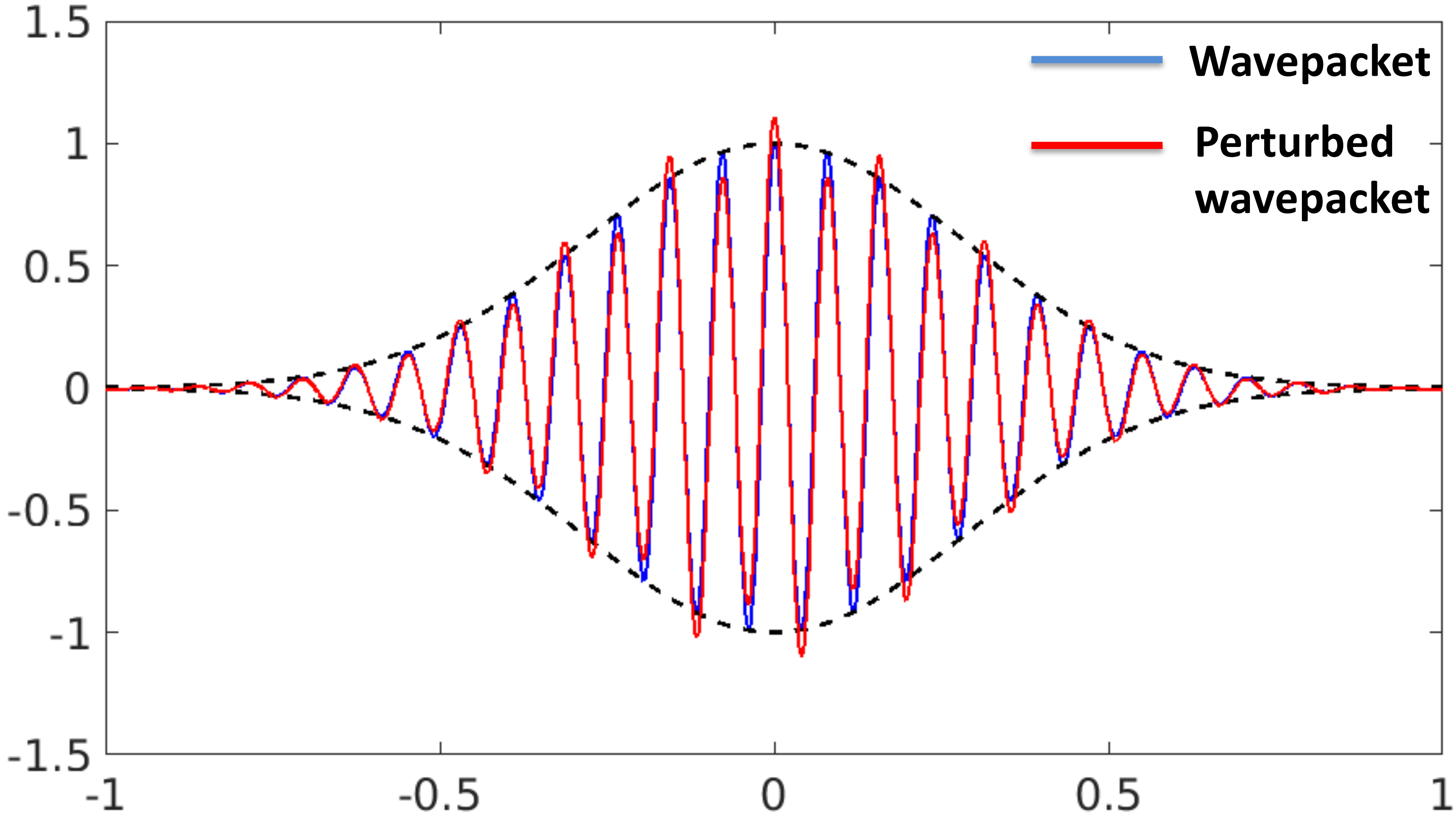

Wei & Freund (2006)

- Compressible shear layer

Uncontrolled

Controlled

→ Acoustically controlled simulation is 11dB quieter

Far-field acoustic spectra

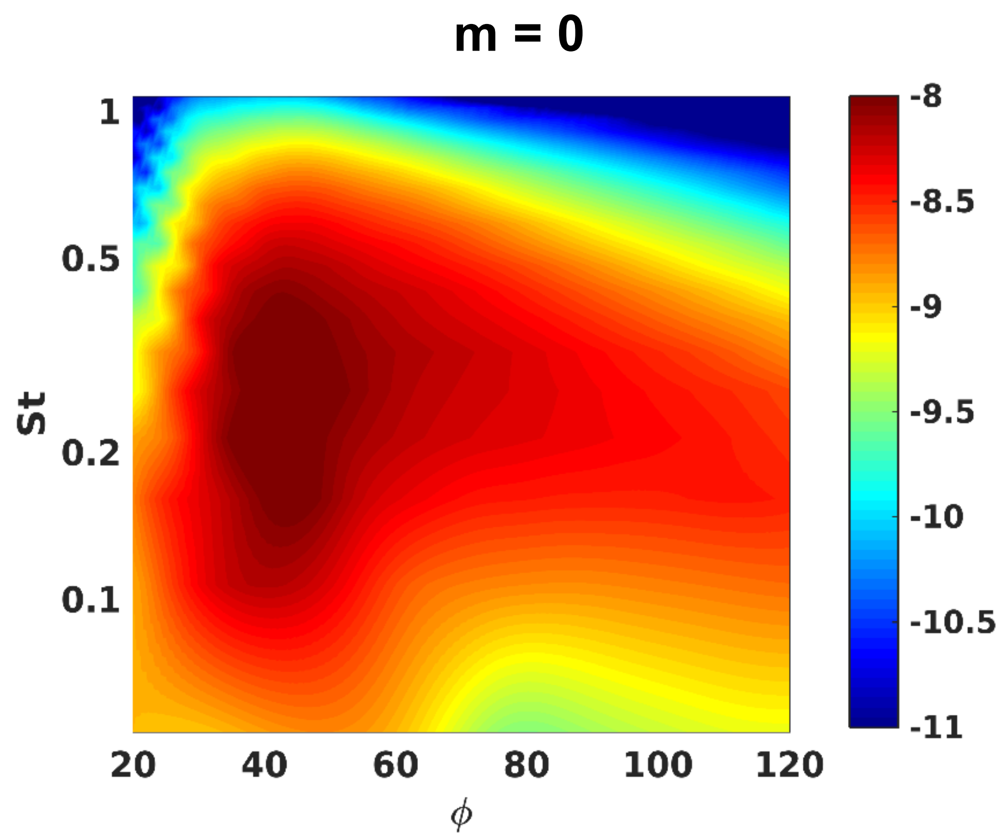

- Input-output analysis shows similar spectra to those obtained by the similarity wavepacket model
- But, the spectrum does not broaden with respect to frequency at high angles

Higher azimuthal modes

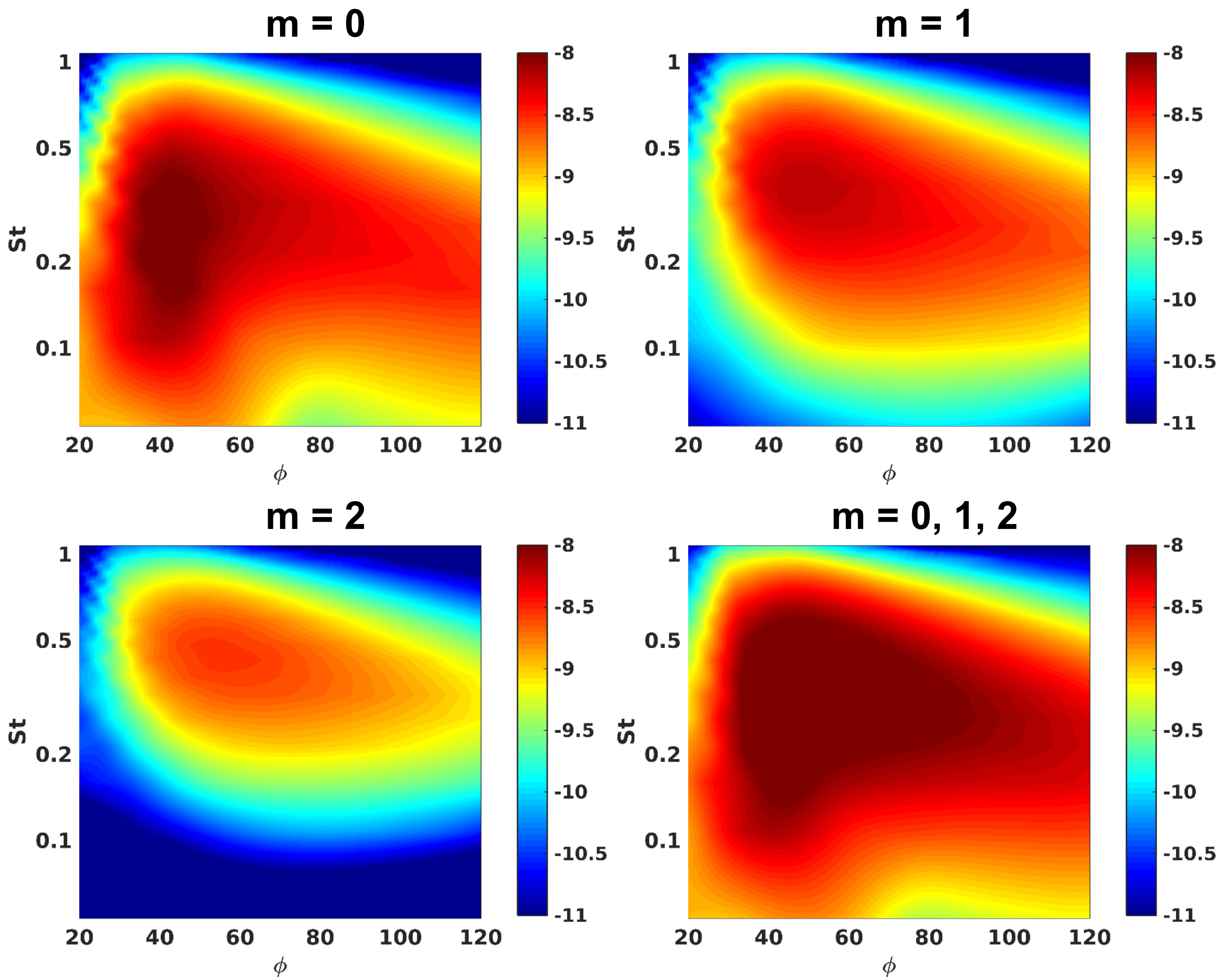

Single observer angle

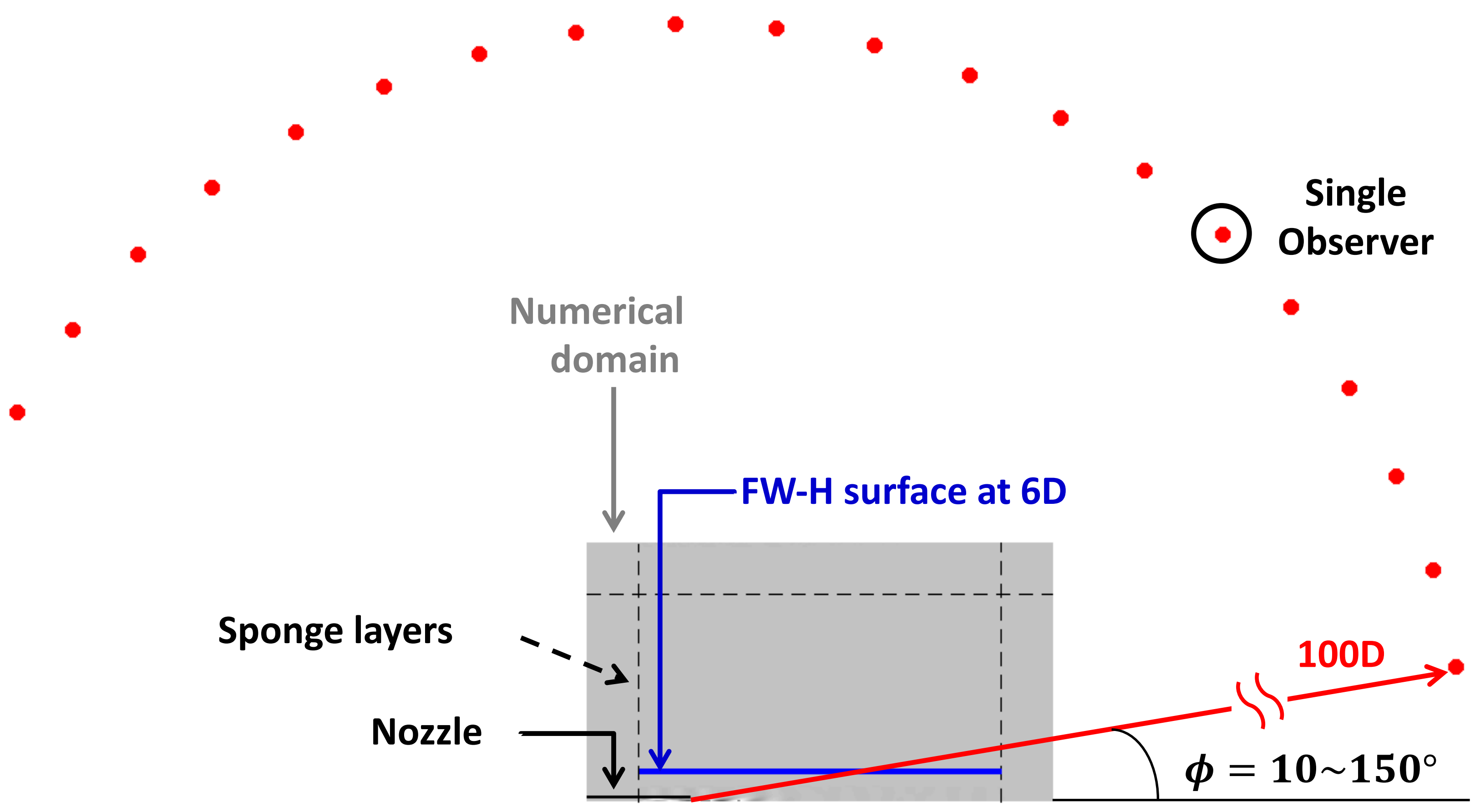

(Jeun & Nichols, AIAA Paper 2018)

Optimal input modes (St = 0.59)

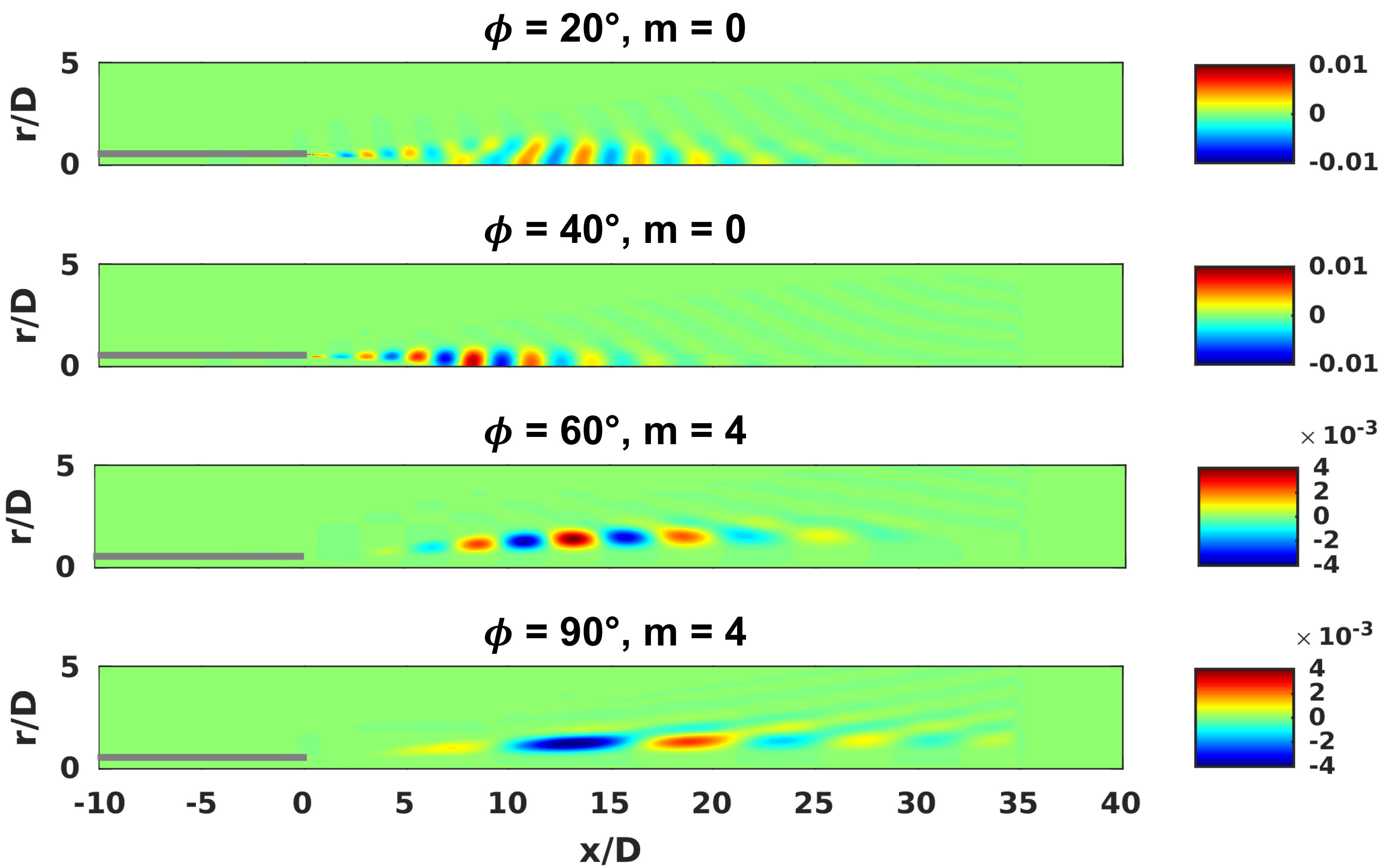

Directivity at 100D (m = 0)

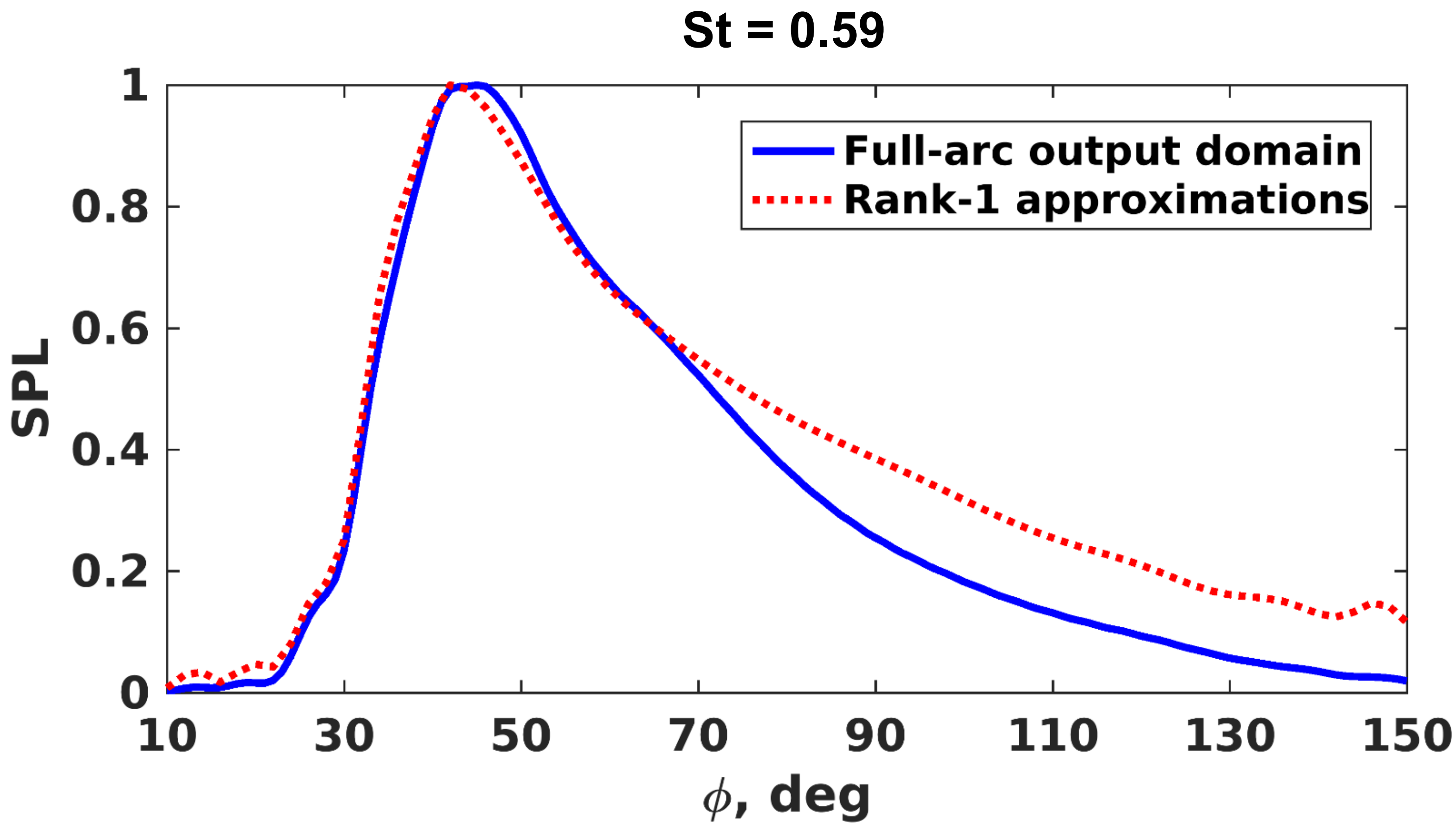

Dynamic acoustic source modeling

- Can I/O analysis reproduce forcing statistics that provide far-field pressure covariance consistent with high-fidelity LES?
- We may design a filter that introduces dynamical modifications to the linearized operator (Zare et al. 2018)

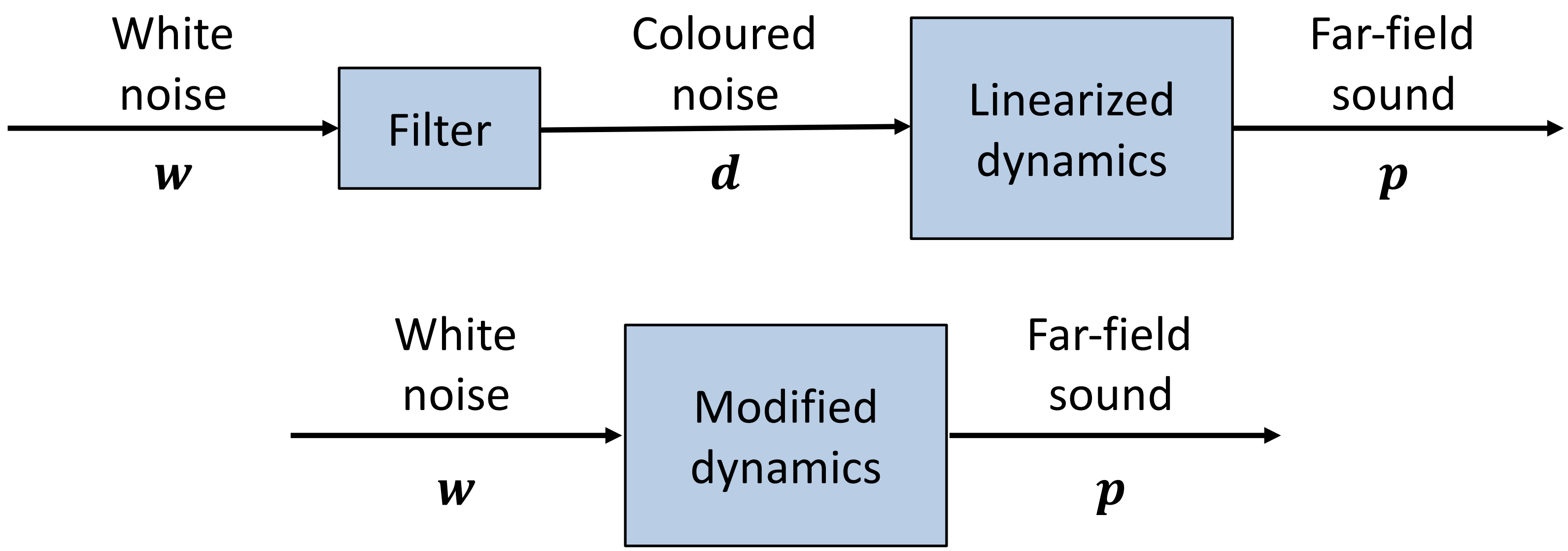

(Zare, Jeun, Nichols, & Jovanovic, APS DFD 2018)

Reduced-order model

- To reduce computational effort, a reduced-order model for I/O behavior of jet noise is necessary
- Method of snapshots
  - Collects snapshots of impulse responses of the direct/adjoint systems
  - Constructs observability/controllability Gramians
  - Recovers balanced modes via SVD

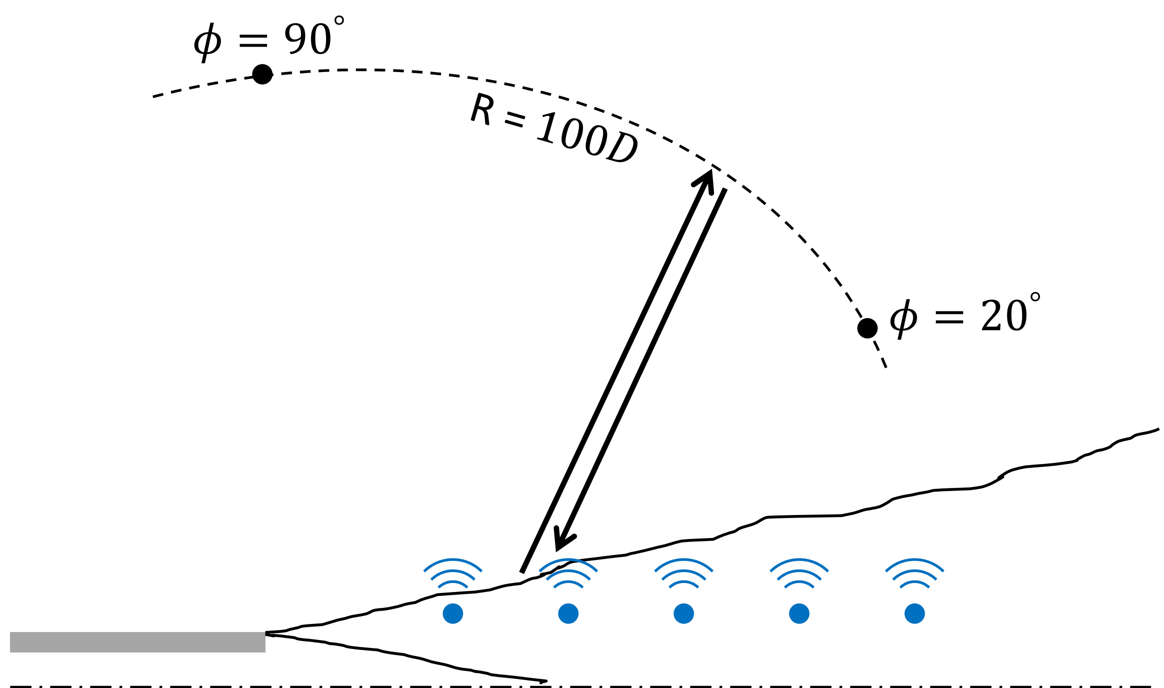

Future applications

- High-fidelity LES data may be decomposed into acoustic, hydrodynamic, and thermal components
  - Doak, JSV 1989; Unnikrishnan & Gaitonde, JFM 2016

$$\rho \boldsymbol{u} = \overbrace{\overline{\boldsymbol{B}} + \boldsymbol{B}'}^{\text{Hydrodynamic}} - \nabla\psi', \quad \nabla\cdot\overline{\boldsymbol{B}} = 0, \quad \nabla\cdot\boldsymbol{B}' = 0,$$

$$\psi' = \underbrace{\psi'_A}_{\text{Acoutic}} + \underbrace{\psi'_T}_{\text{Thermal}}$$

- Does input modes reproduce the **acoustic** component of the source terms?

Future applications

- I/O analysis of complex nozzles
  - Effect of complicated upstream turbo-machinery in a real jet engine

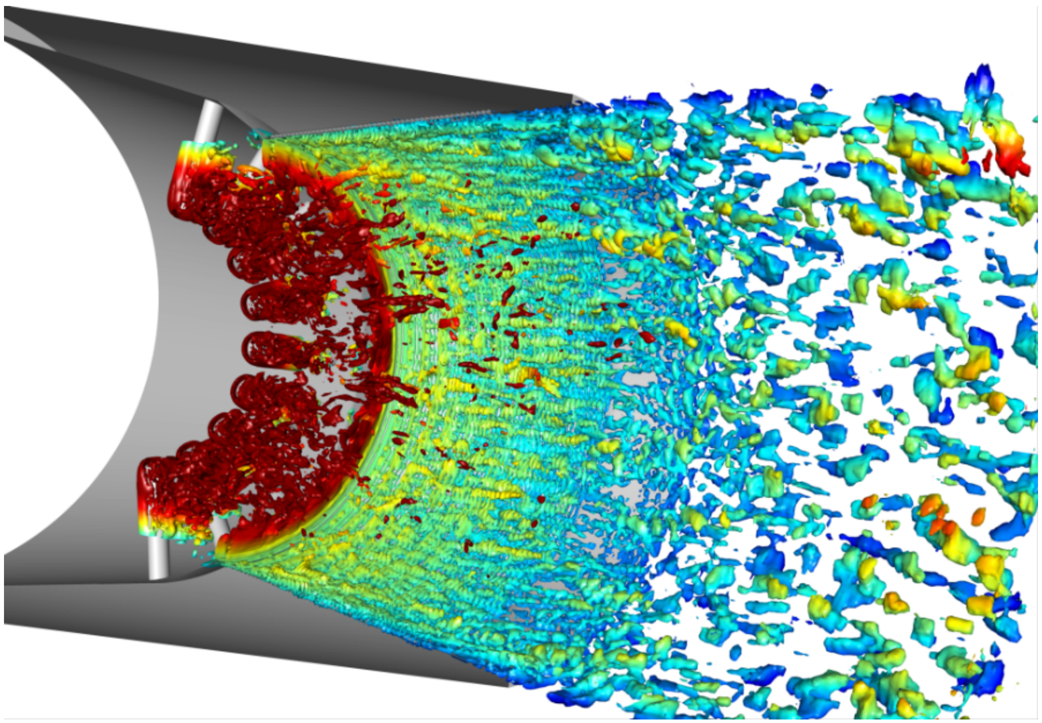

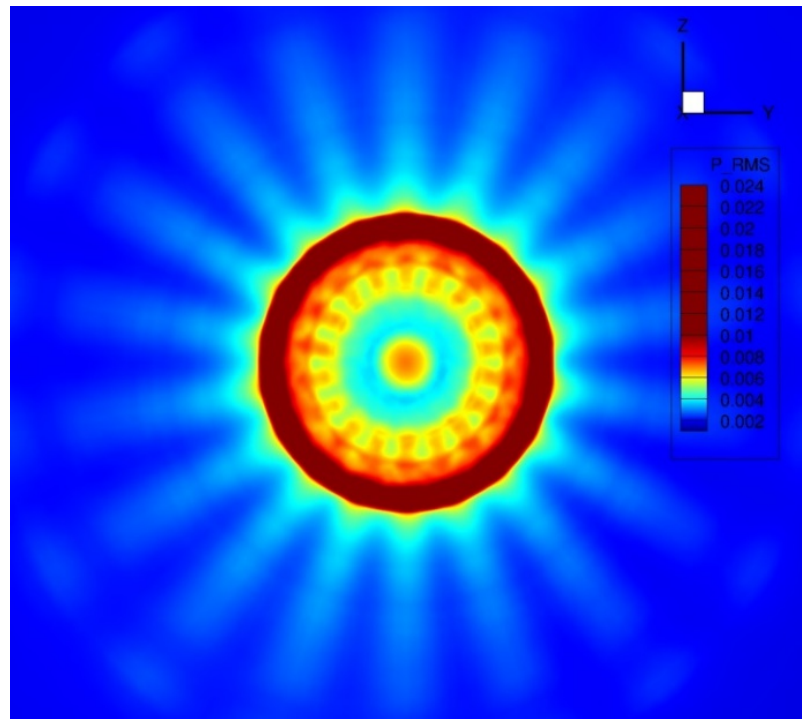

(Dahl, Jeun & Nichols, AIAA Paper 2015)

Future applications

- I/O analysis of complex nozzles

"Chevrons" reduce noise

Future applications

- Linear instabilities evolving on a time-varying base flow
  - Jets controlled by plasma actuators

$$q = \bar{q}(\boldsymbol{x}, \boldsymbol{t}) + q'(\boldsymbol{x}, t)$$

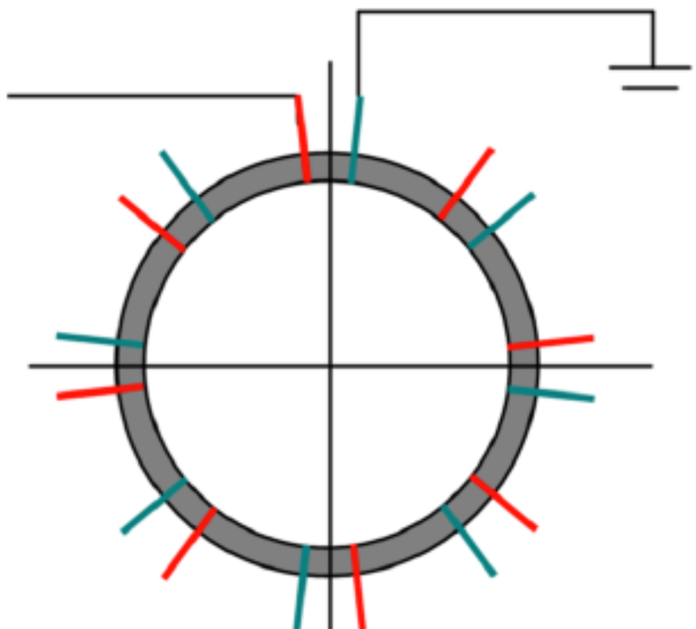

Ceramic nozzle extension with 8 pairs of electrodes

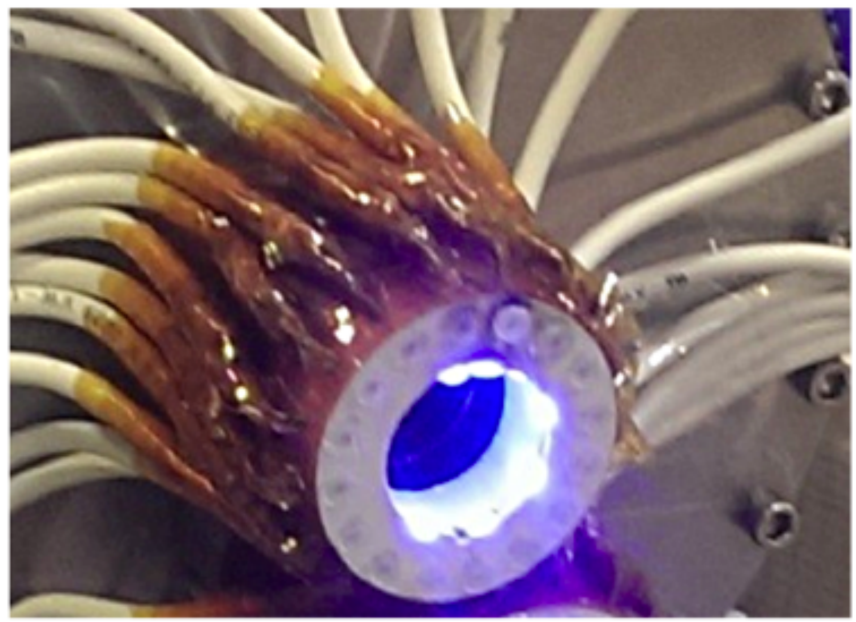

(Samimy, Webb, & Crawley, AIAA J 2018)

Future applications

- Screeching of twin jets
  - High-amplitude tonal components in imperfectly expanded jets
  - Coupling of two jet plumes, mode-switching, etc.

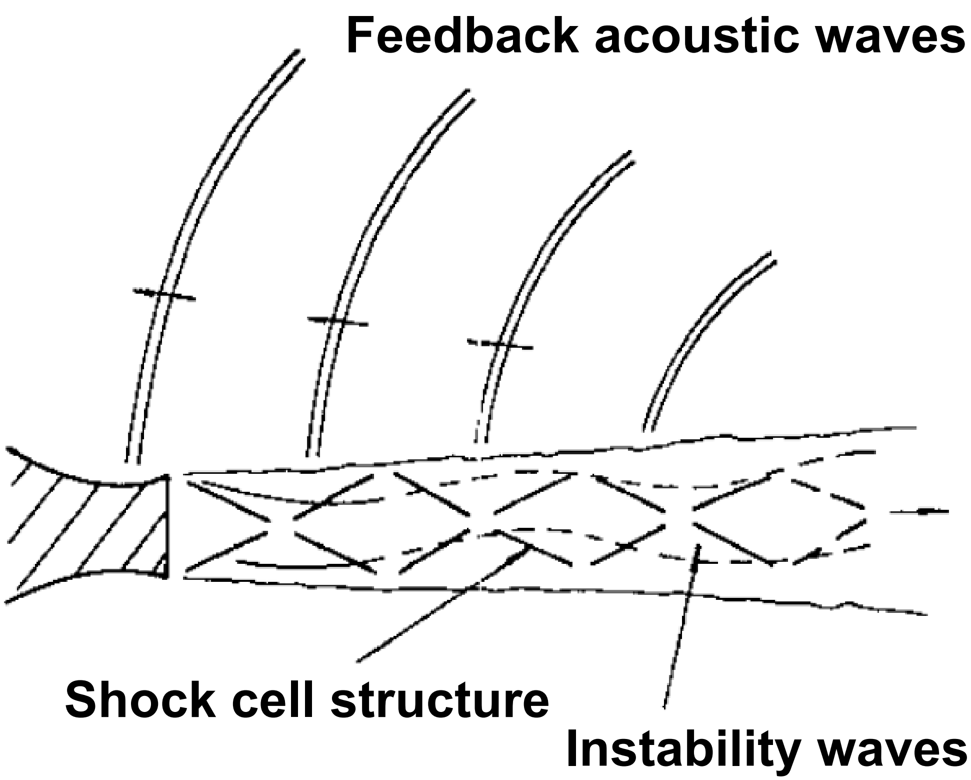

(Tam, ARFM 1995)

Future applications

- Physics-based reduced-order models by studying:
  - Sensitivity of nozzle upstream boundary conditions
  - Sensitivity of nozzle exit shape

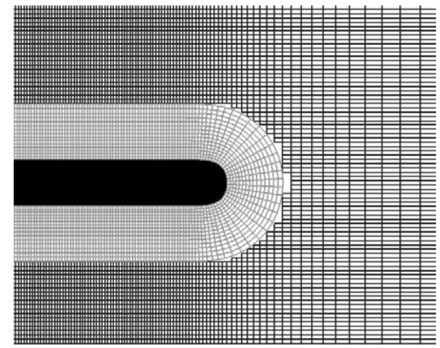

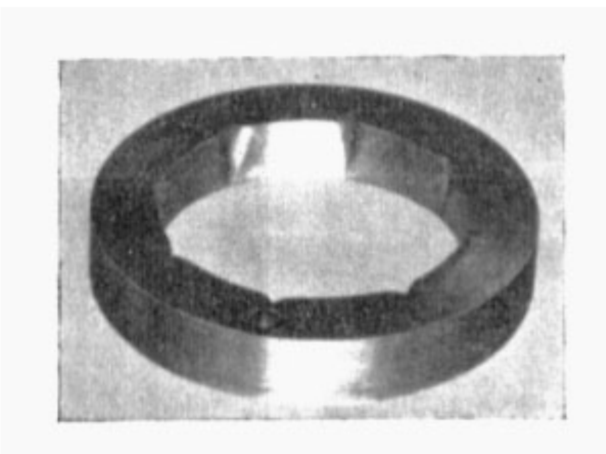

(Powell 1994)

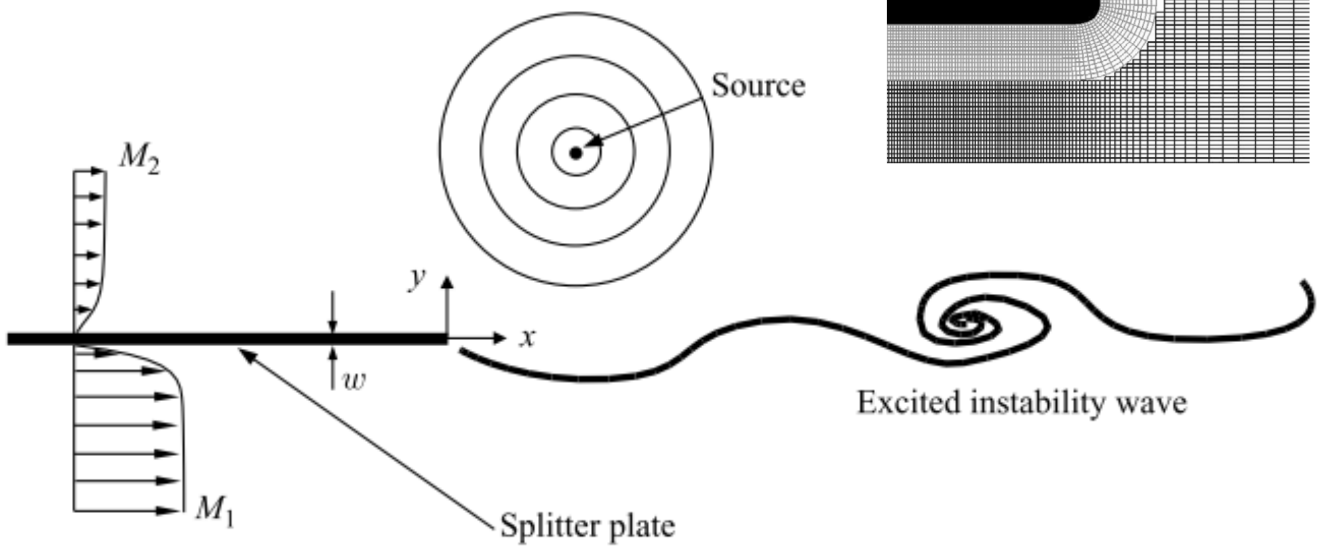

(Barone & Lele 2015)

Summary

- I/O analysis produces optimal and sub-optimal modes
  - I/O modes are observed in LES
- Input modes make physical sense
  - Optimal input modes are similarity wavepackets
  - Sub-optimal modes describe decoherence
  - Optimal mode for subsonic jets connected to subharmonic jitter
- I/O analysis recovers frequency/azimuthal mode dependence, leading to broadened spectra at high observer angles
- Single observer results reveal wavepackets at all angles
- Sideline noise may be explained by coherent mechanisms (Papamoschou 2011, Jordan & Colonius 2013)
- Separation of input sources and output farfield measurements is key

M_j = 0.9 isothermal jet (m=0)

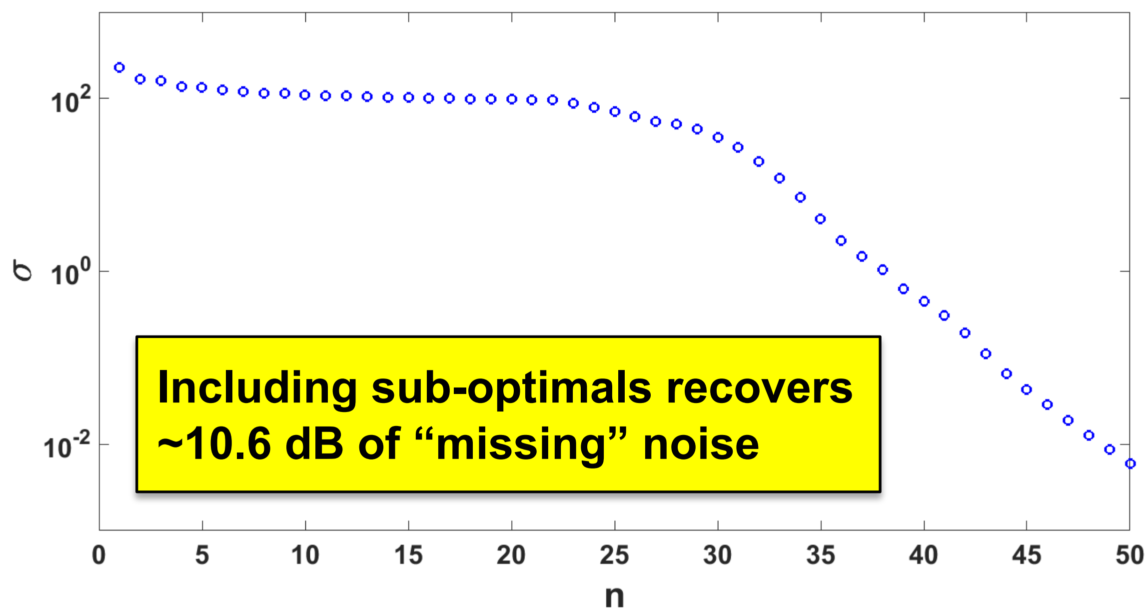

Output modes

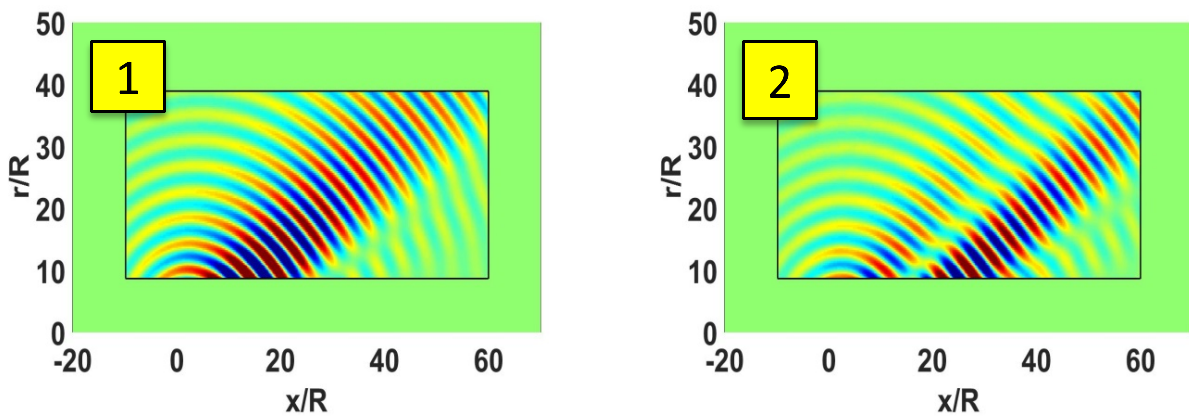

A small wrinkle…

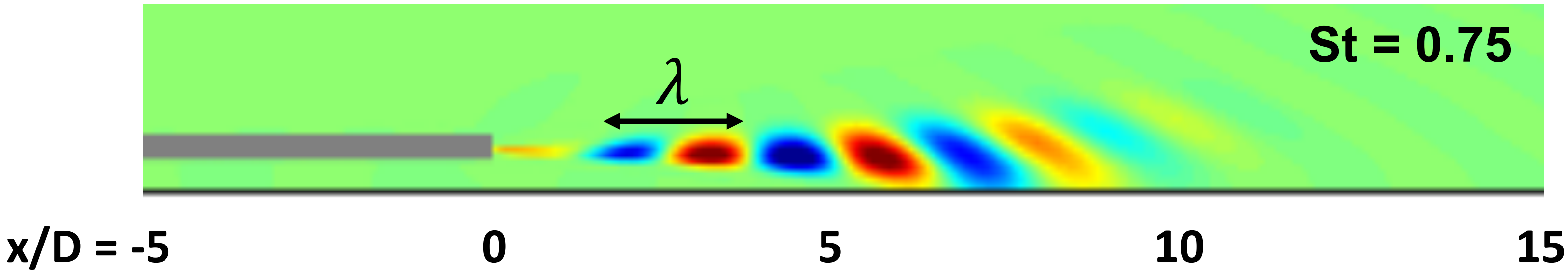

$$c_{phase} = \frac{\lambda}{D} St = \frac{2}{1}(0.75) = 1.5$$

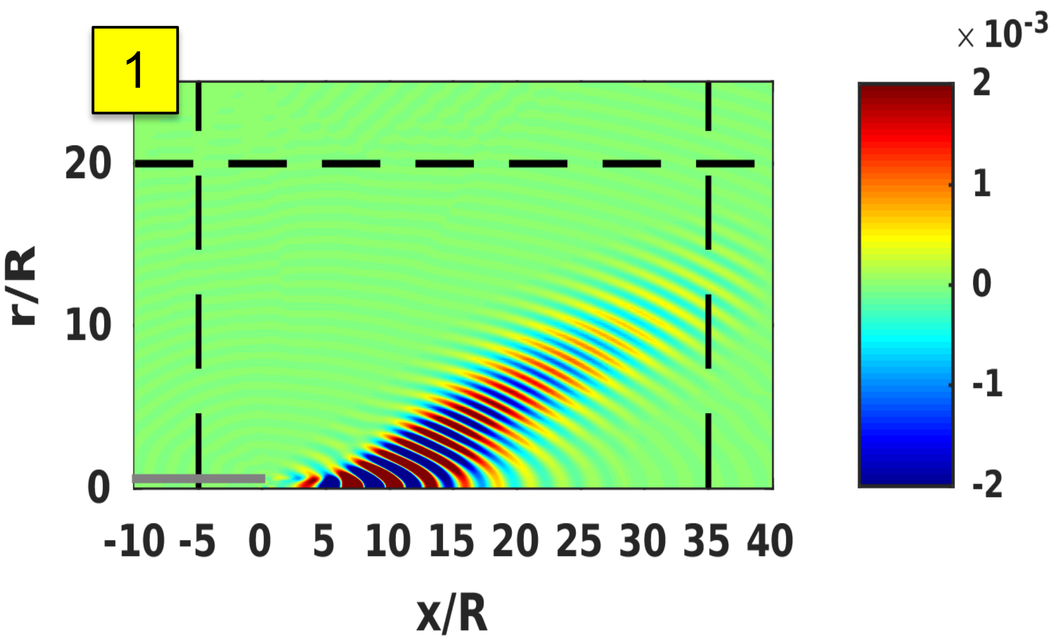

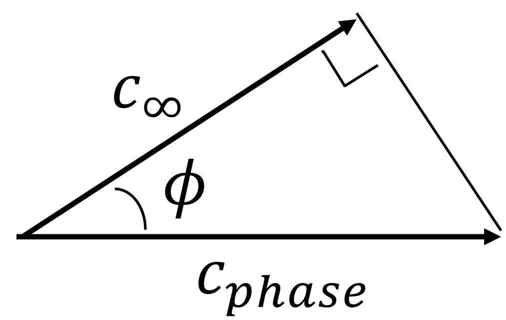

$$\phi = cos^{-1}\left(\frac{1/0.9}{1.5}\right) = 42$$

Decoherence

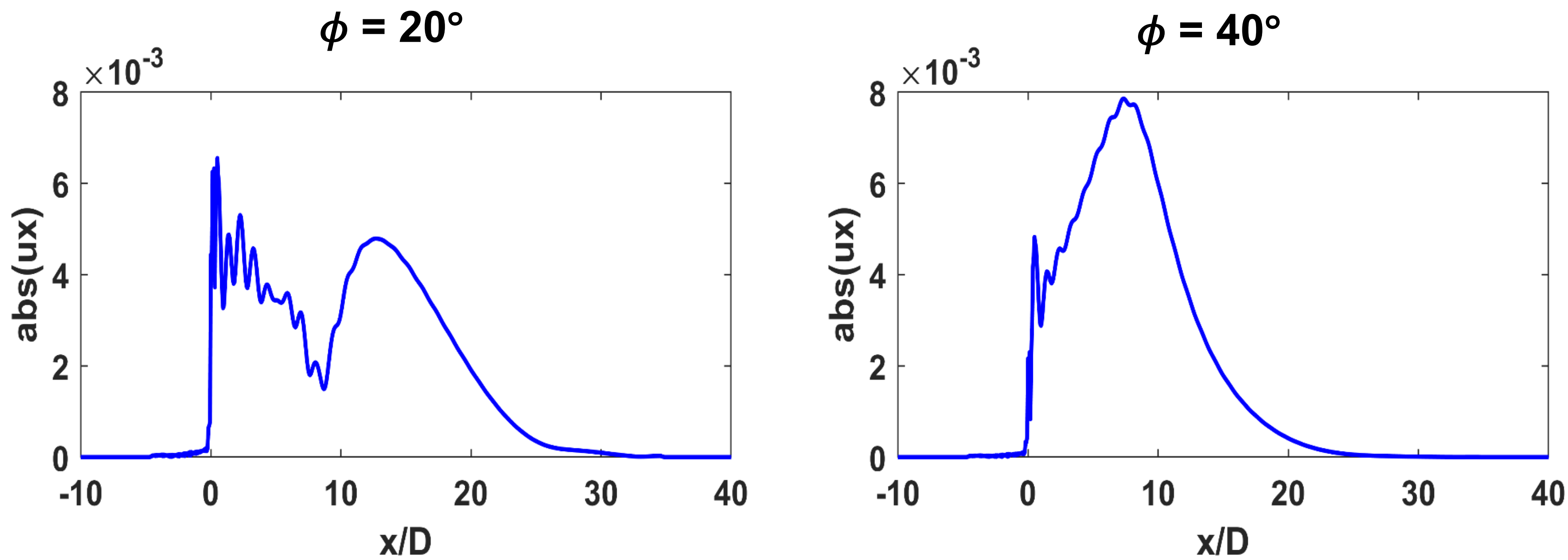

- At low radiation angles, the optimal input mode resembles a sub-optimal mode for the full-arc
  - → At this angle, jet radiates noise by a decoherence mechanism

Compactness & acoustic efficiency

- At high angles, the input mode still recovers wavepackets
  – Sideline noise also may be explained by non-compact sources

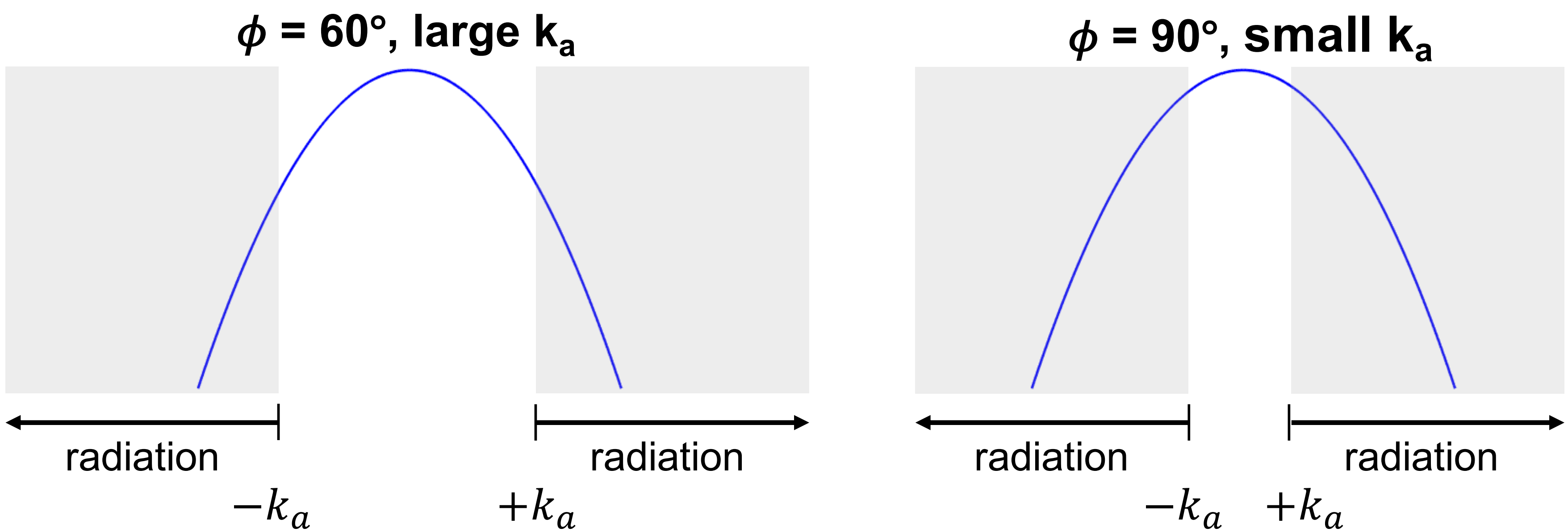

- Wavepacket envelope appears more compact as radiation angle increases
  → Enhances radiative efficiency (Obrist 2009; Serre et al. 2015)

Method of snapshots

- Collects snapshots of impulse responses of the direct / adjoint systems

$$X = [e^{At_1}B, e^{At_2}B, \cdots, e^{At_r}B]\sqrt{\Delta_r},$$
$$Y = \left[e^{A^+t_1}C^+, e^{A^+t_2}C^+, \cdots, e^{A^+t_r}C^+\right]\sqrt{\Delta_r}$$

- Constructs observability / controllability Gramians

$$P \approx XX^H M \qquad \mathrm{Q} \approx YY^H M$$

- Recovers the direct / adjoint balanced modes via SVD

$$Y^H MX = U\Sigma V^H$$

$$T = XV\Sigma^{-1/2} \quad S = YU\Sigma^{-1/2}$$

FW-H method in time domain

- Near-field flow data are projected to far-field sound via the FW-H method in time domain
- FW-H method is implemented within I/O analysis framework

$$4\pi p' = \int_S \left[\frac{\rho_0(\dot{U}_i n_i + U_i \dot{n}_i)}{r|1-M_r|^2}\right]_{ret} dS + \int_S \left[\frac{\rho_0 U_i n_i K}{r^2|1-M_r|^3}\right]_{ret} dS$$

$$+\frac{1}{c}\int_S \left[\frac{\dot{F}_i \hat{r}_i}{r|1-M_r|^2}\right]_{ret} dS + \int_S \left[\frac{F_i \hat{r}_i - F_i M_i}{r^2|1-M_r|^2}\right]_{ret} dS + \int_S \left[\frac{F_i \hat{r}_i K}{r^2|1-M_r|^3}\right]_{ret} dS$$

$$\approx \frac{1}{c}\int_S \left[\frac{\rho_0 \dot{u}_n}{r}\right]_{ret} dS + \frac{1}{c}\int_S \left[\frac{\dot{p}_n \hat{r}_i}{r}\right]_{ret} dS + \int_S \left[\frac{p_n \hat{r}_i}{r^2}\right]_{ret} dS$$

where

$$U_i = u_i + [(\rho/\rho_0) - 1](u_i - v_i)$$

$$K = \dot{M}_i \hat{r}_i r + M_r c - M^2 c$$

$$F_i = L_{ij} n_j \qquad L_{ij} = p\delta_{ij} + \rho u_i (u_i - v_i)$$